A human-based multi-gene signature enables quantitative drug repurposing for metabolic disease

James A Timmons[1,2]*, Andrew Anighoro[3], Robert J Brogan[4], Jack Stahl[5], Claes Wahlestedt[5], David Gordon Farquhar[2], Jake Taylor-King[3], Claude-Henry Volmar[5], William E Kraus[6], Stuart M Phillips[7]

[1]William Harvey Research Institute, Queen Mary University of London, London, United Kingdom; [2]Augur Precision Medicine LTD, Stirling, United Kingdom; [3]Relation Therapeutics LTD, London, United Kingdom; [4]Fiona Stanley Hospital, Perth, Australia; [5]Center for Therapeutic Innovation, Miller School of Medicine, University of Miami, Miami, United States; [6]School of Medicine, Duke University, Durham, United States; [7]Faculty of Science, Kinesiology, McMaster University, Hamilton, Canada

Abstract Insulin resistance (IR) contributes to the pathophysiology of diabetes, dementia, viral infection, and cardiovascular disease. Drug repurposing (DR) may identify treatments for IR; however, barriers include uncertainty whether in vitro transcriptomic assays yield quantitative pharmacological data, or how to optimise assay design to best reflect in vivo human disease. We developed a clinical-based human tissue IR signature by combining lifestyle-mediated treatment responses (>500 human adipose and muscle biopsies) with biomarkers of disease status (fasting IR from >1200 biopsies). The assay identified a chemically diverse set of >130 positively acting compounds, highly enriched in true positives, that targeted 73 proteins regulating IR pathways. Our multi-gene RNA assay score reflected the quantitative pharmacological properties of a set of epidermal growth factor receptor-related tyrosine kinase inhibitors, providing insight into drug target specificity; an observation supported by deep learning-based genome-wide predicted pharmacology. Several drugs identified are suitable for evaluation in patients, particularly those with either acute or severe chronic IR.

Editor's evaluation

This study reports the discovery of EGFR related tyrosine kinase inhibitors as agents that could potentially be repurposed to counteract metabolic disturbances arising from insulin resistance. The authors have used a computational approach to define a gene signature, which was then inputted to identify 130 compounds that interacted with pathways involved in insulin resistance. Important clinical implications may eventually follow from these studies.

Introduction

Systemic insulin resistance (IR) is a multi-organ pathophysiological state and an early characteristic of type 2 diabetes mellitus (T2DM). IR contributes to the pathobiology of neurodegeneration (*Norambuena et al., 2017*), heart failure (*Wamil et al., 2021*) and viral infections, such as COVID-19 (*Ceriello et al., 2020*; *Donath, 2021*). Several T2DM drug treatments *indirectly* reduce IR following improved metabolic homeostasis, making them candidate treatments for various diseases (*Donath, 2021*; *Everett et al., 2018*; *Norambuena et al., 2017*). Drug repurposing (DR) aims to accelerate

eLife digest Developing a new drug that is both safe and effective is a complex and expensive endeavor. An alternative approach is to 'repurpose' existing, safe compounds – that is, to establish if they could treat conditions others than the ones they were initially designed for. To achieve this, methods that can predict the activity of thousands of established drugs are necessary.

These approaches are particularly important for conditions for which it is hard to find promising treatment. This includes, for instance, heart failure, dementia and other diseases that are linked to the activity of the hormone insulin becoming modified throughout the body, a defect called insulin resistance. Unfortunately, it is difficult to model the complex actions of insulin using cells in the lab, because they involve intricate networks of proteins, tissues and metabolites.

Timmons et al. set out to develop a way to better assess whether a drug could be repurposed to treat insulin resistance. The aim was to build a biological signature of the disease in multiple human tissues, as this would help to make the findings more relevant to the clinic. This involved examining which genes were switched on or off in thousands of tissue samples from patients with different degrees of insulin resistance. Importantly, some of the patients had their condition reversed through lifestyle changes, while others did not respond well to treatment. These 'non-responders' provided crucial new clues to screen for active drugs.

Carefully piecing the data together revealed the molecules and pathways most related to the severity of insulin resistance. Cross-referencing these results with the way existing drugs act on gene activity, highlighted 138 compounds that directly bind 73 proteins responsible for regulating insulin resistance pathways. Some of the drugs identified are suitable for short-term clinical studies, and it may even be possible to rank similar compounds based on their chemical activity.

Beyond giving a glimpse into the complex molecular mechanisms of insulin resistance in humans, Timmons et al. provide a fresh approach to how drugs could be repurposed, which could be adapted to other conditions.

the discovery and reduce the costs of new treatments. Multiple evolving strategies are being trialled, including mining of medical records, development of large databases of drug-gene interactions (*Subramanian et al., 2017*) and virtual compound screening (*Himmelstein et al., 2017*). Drug transcriptome responses in cells represent one of the most extensive resources (*Subramanian et al., 2017*), while transcriptomics is also an ideal technology to capture complex biological processes in human tissues (*Jenkinson et al., 2016*; *Timmons et al., 2018*; *Timmons et al., 2005*). Effectiveness at reversing of the molecular responses to disease (*Wagner et al., 2015*) helps to predict drug efficacy in cancer (*Brown and Patel, 2018*; *Iorio et al., 2018*; *Karatzas et al., 2017*; *Wang et al., 2016*). Successful application of DR specifically to oncology may reflect that drug profiles are typically generated in tumour cell lines (*Subramanian et al., 2017*) and that barriers to clinical validation can be lower compared with many other diseases.

Identifying informative disease signatures for DR in cells is challenging (*Chen et al., 2020*; *Karatzas et al., 2017*; *Regan-Fendt et al., 2019*), particularly when no positive controls exist (*Williams et al., 2019*). Currently, there are no reliable human cellular models for systemic IR, while it remains unclear if multi-gene assays can capture quantitative pharmacological relationships suitable for optimising drug design. However, clinically effective drugs typically target several proteins, many of which are unknown (*Keenan et al., 2018*), highlighting the limitations of single-target drug development programmes. Network modelling and deep learning (DL) have been utilised to connect the pharmacological properties of active drugs to their protein targets (*Woo et al., 2015*; *Zeng et al., 2020*). For IR we also have effective non-drug treatments (*Nakhuda et al., 2016*; *Slentz et al., 2016*; *Timmons et al., 2018*; *Phillips et al., 2017*), and this enabled production of a novel human-based IR-DR assay – using more than 2000 tissue profiles generated in our laboratories (*Nakhuda et al., 2016*; *Slentz et al., 2016*; *Timmons et al., 2018*) and one other (*Civelek et al., 2017*). Performance of the present RNA-based multi-gene assays was judged against positive control in vivo drug signatures (*Stathias et al., 2020*), genome-wide association (*Lotta et al., 2017*; *Vujkovic et al., 2020*) and blood proteome-based assays (*Gudmundsdottir et al., 2020*). Validation of the in vitro results for >2500 drugs (*Subramanian et al., 2017*) relied on a variety of protein, drug- and disease-centric (*Parisi et al., 2020*) criteria:
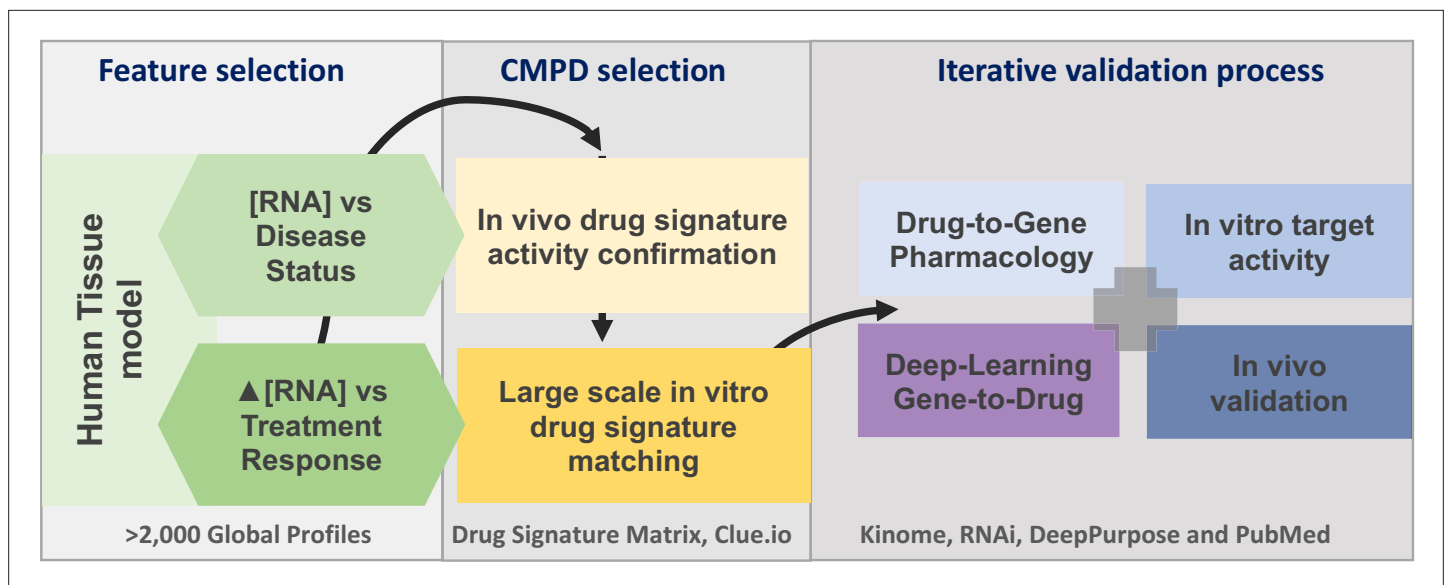
Figure 1. The project analysis process. The three major phases of the project are defined by the grey boxes. A limited number of gene signatures were considered (four) to limit false-positive associations. The compound (CMPD) selection phase first confirmed that the drug repurposing signature provided valid matches with in vivo positive control drugs, and then a full list of in vitro active drug matches was generated. The third phase was an iterative process in that validation was considered on several levels. We utilised four main independent validation strategies, incorporating multiple data sources, to demonstrate that the insulin resistance drug repurposing (IR-DR) signature produced a high rate of likely true-positive drugs that would reverse IR.

DL-based modelling of drug-to-protein interactions; targeted gene knock down; and published evidence that the drug reduced IR in vivo (*Figure 1*).

Results and discussion
Feature selection and in vivo validation of novel IR-DR assays

Homeostasis model assessment version 2 (HOMA2-IR) was used to quantify IR (*Wallace et al., 2004*). RNA biomarkers consistently related to fasting IR ('disease') across tissues were combined with those regulated in common across tissues following lifestyle-based reversal of IR ('treatment'). Biomarkers were ranked based on consistent direction and strength of association across two major human organs targeted by insulin (human adipose and muscle) because most orally dosed drugs will act systemically. Quantitative network modelling (*Song and Zhang, 2015*) was used to rank genes for their tissue-based hub connectedness (*Appendix 1—figure 1*). In the present study, we considered the performance of only four RNA-based IR-DR assays (*Appendix 1—figure 1*; *Ganter et al., 2006*); testing their ability to match the in vivo directionality of positive controls, thiazolidinedione (TZD) and oestrogen, expression signatures correctly (*Hevener et al., 2018*; *Sears et al., 2009*). The top-scoring RNA signature (Signature 3A from *Appendix 1—figure 1*) was a statistically ranked combination of disease- and treatment-associated genes (n = 120 genes) outranked selection by hub connectedness, recapitulated cellular gene expression patterns indicative of TZD treatment responses in vivo in muscle (moderated Z-score, p<0.0000008, *Appendix 1—figure 2*) and is referred to as the IR-DR signature/assay hereafter (*Appendix 1—figure 1*). Lack of superiority for the assay designed using hub connectedness may be considered at odds with other studies (*Cheng et al., 2012*) but could reflect that inclusion of multi-tissue treatment response biomarkers supersedes any benefit of using network weighting. Several Genome-wide Association Study (GWAS) IR and T2DM (*Lotta et al., 2017*; *Vujkovic et al., 2020*)-derived signatures (e.g. Signature 4, *Appendix 1—figure 1*) were considered but were unable to match positive control drugs in vivo. The T2DM blood proteome signature (*Gudmundsdottir et al., 2020*) had a weak association with one positive control drug. Protein-level network interactions formed by each list (*Appendix 1—figure 1*) were distinct (*Appendix 1—figure 2*) and were only possible to partially recreate from existing databases (*Li et al., 2018a*).

IR-DR assay identifies drugs and pathways with established links with insulin signalling

The largest available database of in vitro drug signatures (*Subramanian et al., 2017*) was used to identify cell-type agnostic drug responses. To achieve this, we utilised aggregated scores (the maximum quantile statistic from the within-cell line-normalised scores) from across nine human cell lines. This approach also increases the sample size per drug by at least ninefold, making any inferences more reliable (*Subramanian et al., 2017*). At the request of a reviewer, we provide results from individual cells (Table S3 *Appendix 1—figure 3*); however, we caution that these within-cell rank-order values are known to be less robust (*Subramanian et al., 2017*; *Xu et al., 2018*). Critically, we noted that members of each drug 'class' (drugs sharing a nominal primary protein target in common) were segregated with either active or neutral IR-DR scores, with extremely few drug classes having both positive- and negative-scoring compounds. Only 10% of the database matched the IR-DR signature (n = 254, *Appendix 1—figure 3* and Table S3), and 138 compounds (after excluding assay codes with ambiguous compound labels) positively regulated the IR-DR signature (potential treatments), 45% of which were kinase inhibitors (*Appendix 1—figure 4*). Most negative acting drugs targeted tubulin and cell cycle proteins or were pro-inflammatory agents (*Appendix 1—figure 5*). Positive and negative acting compounds did not differ in average physiochemical properties (*Appendix 1—figure 6*), while assays based on GWAS-selected genes for IR (*Lotta et al., 2017*; *Vujkovic et al., 2020*) and T2DM produced no discernible pattern of in vitro hits.

The pharmacology of the 138 positive compounds indicated that a substantial number of targeted aspects of insulin signalling were known, empirically, to reverse IR in vivo (*Table 1*). Compounds identified varied in nature from inhibitors of glucosylceramide synthase, which reverses IR and fatty liver disease (*Aerts et al., 2007*; *Herrera Moro Chao et al., 2019*), to 10 mTOR inhibitors. The mTOR complex, mTORC1, coordinates a negative feedback loop on insulin signalling, for example, through activation of GRB10 or via S6K1 (*Um et al., 2004*). mTORC1 signalling is also regulated by protein kinase C (PKC) (*Zhan et al., 2019*), and specific PKC isoforms are dysregulated in ageing, metabolic, neurodegenerative and inflammatory diseases (*Li et al., 2015*; *Sajan et al., 2018*; *Sharma et al., 2019*). We observed that the broad-spectrum PKC inhibitor, bisindolylmaleimide I, induced a strong positive IR signature score (+87) and the related compound, ruboxistaurin, reverses IR in vivo (*Guo et al., 2020*; *Naruse et al., 2006*). In contrast, bisindolylmaleimide IX, a 20-fold more potent broad-spectrum PKC inhibitor, was inactive in the IR-DR assay, probably reflecting its greater non-specific pharmacology (against other kinase families). Three so-called PKC activators (*French et al., 2020*; *Lee et al., 2020*) induced *negative* IR-DR scores (phorbol-12-myristate-13-acetate = –87, ingenol = –96 and prostratin = –97). RNAi targeting of individual PKC isoforms (clue.io) demonstrated that the IR-DR assay was sensitive to specific PKC isoformactivity. While >95% of all RNAi assays produced no significant scores, knock-down (KD) of PKC-beta (+74) and PKC-theta (+97) yielded positive IR-DR scores, while loss of PKC-alpha (–75) and -eta (–75) produced negative IR-DR scores and overexpression (OE) of PKC-alpha was positive scoring (+85). The multi-gene IR-DR assay therefore identifies numerous true-positive drugs (*Table 1*) and reflects isoform-specific activity, strongly validating the cell-agnostic aggregation methodology.

Identification of the active drug-protein targets through single-gene targeting and network biology

The 138 positive scoring IR-DR drugs target 1007 proteins (*Mendez et al., 2019*; *Moret et al., 2019*). Of these, 465 genes had single-gene KD or OE scores, aggregated across 6–9 cell lines (*Appendix 1—figure 7*). Seventy-three targets (15.7%) yielded a significant IR-DR score; double the assay hit rate (p<0.0001, see Methods and *Figure 2*). Predictably, due to input bias (*Timmons et al., 2015*), these targets regulated 'peptidyl-serine phosphorylation-related processes' (q-value $<1 \times 10^{-23}$). None belonged to the IR-DR gene signature (*Appendix 1—figure 8*), but they did belong to numerous common pathways (*Appendix 1—figure 8*). These observations are consistent with the idea that an effective DR signature captures the pathway biology of the disease and/or treatment (*Brown and Patel, 2018*; *Chen et al., 2020*; *Karatzas et al., 2017*; *Keenan et al., 2018*; *Regan-Fendt et al., 2019*; *Wagner et al., 2015*; *Woo et al., 2015*) but does not necessarily include the nominal drug targets (*Figure 2*).

Table 1. Examples of the major drug classes producing a positive insulin resistance-drug repurposing (IR-DR) score and associated literature evidencing efficacy. In vivo refers to evidence for in vivo validation of the drug and/or its target proteins.

Pathway	Example drug	Biology narrative	In vivo	Example literature
ATPase/cardiac glycoside	Proscillaridin, digoxin	Heart failure drug; possibly mimicking the action of metformin on mitochondria in vitro; senolytic.	No	*Fürstenwerth, 2012; Triana-Martínez et al., 2019*
Calcium channel	Nifedipine	Restores autophagy, improves glucose tolerance and insulin action.	Yes	*Iwai et al., 2011; Koyama et al., 2002; Lee et al., 2019; Sheu et al., 1991*
Calcium/calmodulin signalling	NM-PP1	Insulin signalling upstream of p38; restores ATF6-related autophagy; insulin resistance, diabetes and Alzheimer's pathophysiology.	Yes	*Alfazema et al., 2019; Ozcan et al., 2015; Ozcan et al., 2013; Yin et al., 2017*
Dopamine	L-741626	Central and peripheral role in regulation of glucose tolerance – contradictory/paradoxical behavioural/hepatic agonist/antagonist activity.	Yes	*Amamoto et al., 2006; Fontaine et al., 2020; Kellar and Craft, 2020; Park et al., 2007; Stoelzel et al., 2020*
Tyrosine kinase/ERBB receptor inhibitors	Canertinib, gefitinib, afatinib	Inhibition of EGFR, DDR1, ABL1 and related kinases produces a positive IR-DR score. Extensive data link EGFR and inhibitors of EGFR to insulin resistance and neurodegeneration. Pro-inflammatory signalling via iRHOM2 and MAP3K7; circulating biomarker of insulin resistance and hepatic metabolic disease.	Yes	*Chen et al., 2019; Chiu et al., 2020; Fowler et al., 2020; Kyohara et al., 2020; Li et al., 2018b; Skurski et al., 2020; Vella et al., 2019; Wang et al., 2012; Wu et al., 2017*
Glucocorticoid/anti-inflammatory	Valdecoxib, Spectrum_001832	Anti-inflammatory; various steroidal and non-steroidal anti-inflammatory drugs reduce IR in a variety of models of diabetes/obesity. Excess corticosteroids induce IR.	Yes	*Chakraborti et al., 2010; Chan et al., 2018; Reading et al., 2013*
Glucosylceramide synthase	BRD-K88761633, AMP-DNM	Glycosphingolipid biosynthesis – inhibition treats insulin resistance and fatty liver disease.	Yes	*Aerts et al., 2007; Herrera Moro Chao et al., 2019*
Heat-shock protein 90	Luminespib	ATPase cycle and chaperone function – inhibition improves insulin sensitivity; Hsp90 activated in dementia. Role in INSR turnover and protein phosphatase 5 activation.	Yes	*Imamura et al., 1998; Jing et al., 2018; Shelton et al., 2017; Yang et al., 2005*

Table 1 continued on next page

Table 1 continued

Pathway	Example drug	Biology narrative	In vivo	Example literature
MAPK/MEK/ERK inhibitors	PD-184352, PD-0325901, XMD-892	Multiple roles in insulin signalling and metabolism; inhibitors target multiple kinases.	Yes	*Ozaki et al., 2016; Sharma et al., 2014; Tarragó et al., 2018; Wauson et al., 2013*
mTOR related	AZD-8055, WYE-354, torin-2	Inhibition of mTORC1 activity – including knock-down of RAPTOR – produces a strong positive IR-DR score. In multiple studies, mTOR inhibition reduces age-related metabolic dysfunction.	Yes	*Howell et al., 2017; Jahng et al., 2019; Morita et al., 2013; Nie et al., 2018a; Norambuena et al., 2017; Zhan et al., 2019*
Nicotinamide phosphoribosyltransferase	CAY-10618 (GPP78)	NAMPT (or visfatin) inhibitor which attenuates atherosclerosis in the high-fat-induced insulin resistance model and is anti-inflammatory.	Yes	*Li et al., 2016; Lockman et al., 2010; Travelli et al., 2017*
Phosphodiesterase 5A	MBCQ, sidenafil	PDE5A is negative regulator of insulin, aspects of ageing – potentially via miR-22-3p.	Yes	*Blagosklonny, 2017; Fiore et al., 2018; Fiore et al., 2016; Liu et al., 2019*
Phosphoinositide 3-kinase	AZD-6482, PI-103, GDC-0941	Multiple PI3K inhibitors produce strong positive IR-DR scores. In multiple studies PI3K varies with metabolic dysfunction; however, all kinase inhibitors target multiple related kinases, so specific target unclear.	No	*Chiu et al., 2020; Copps et al., 2016; Wang et al., 2020; Zou et al., 2004*
RAF kinase	AZ-628, vemurafenib	RAF1 is increased in obesity-induced IR, inhibitors can block insulin/AKT1/MAPK signalling in a context-specific manner. AZ-628 also RIP3 inhibitor – anti-arthritis strategy.	No	*MacLaren et al., 2008; Osrodek et al., 2020; Sun et al., 2016*

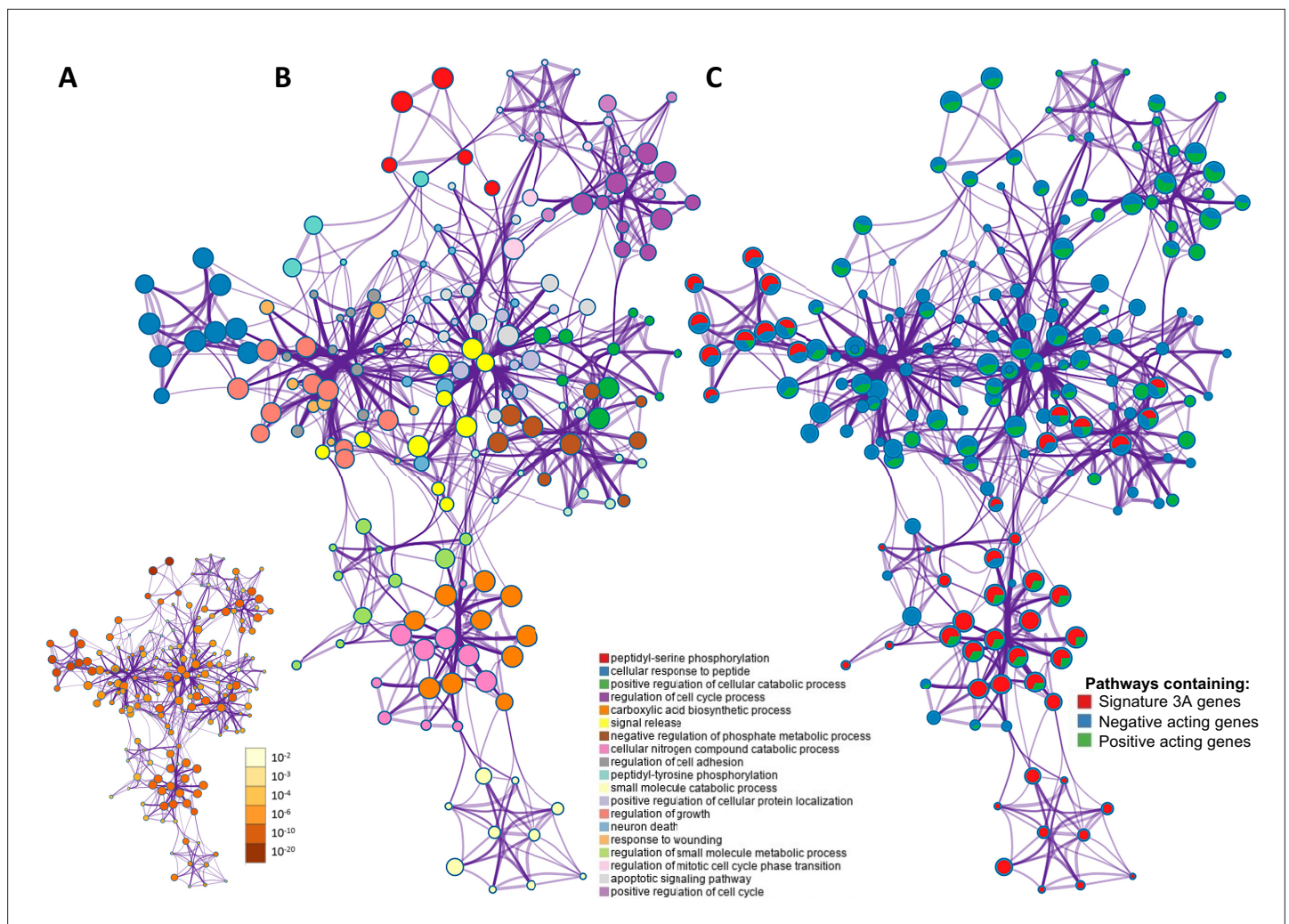EGFR, epidermal growth factor receptor.

Figure 2. The overlap between protein targets of positively acting drugs and the insulin resistance-drug repurposing (IR-DR) input signature. (**A**) A network of significant pathways coloured by p-values, derived from the IR-DR input genes and the 73 validated protein targets of the 150 positively acting drugs. (**B**) Edges represent connected Gene Ontology (GO) biological processes (>0.3), and nodes within each cluster are coloured/named by their most statistically enriched GO term. (**C**) Each node is presented as a pie chart, scaled in size by the total number of terms represented by that (top-scoring) ontology, and with the 'slices' coloured to indicate which gene list the terms originate from. The same network structure is separately colour-coded by list membership to identify when pathways include members of Signature 3A (red), or protein targets which are negative acting genes (blue, where inhibition yields a positive and overexpression yields a negative IR-DR score) or genes appear to be positively acting (green).

Network representation of how these 73 *independently* validated target proteins of active drugs (*Appendix 1—figure 4*) interact with IR-DR signature at a pathway level is presented in *Figure 2*A (Benjamini-Hochberg corrected p-values). The GO terms are scaled by the total number of significant terms and labelled by the top-level category (*Figure 2*B). Coloured orange (*Figure 2*B), a module of the 'carboxylic acid biosynthetic process' pathway contains genes that, when more 'active,' positively modulate the IR-DR signature (Z = 8.3, p=1 × 10^{-9}). Each pathway is also coloured (*Figure 2*C) to indicate whether it contains a known drug target or was part of the IR-DR signature. The IR-DR assay genes formed eight pathway clusters, of which the majority directly contain some RNAi validated protein targets, for example, 'negative regulation of phosphate metabolic process' (coloured brown, q-value 1 × 10^{-7}). As with the analysis of the individual PKC isoforms, there are compelling examples of proteins contributing to metabolic disease, for example, SMAD3 (+87 IR-DR score from OE and −95 IR-DR score from RNAi) is an in vivo-validated IR pathway (*Budi et al., 2019*; *Sun et al., 2015*; *Tan et al., 2011*). However, if multi-gene DR assays are to be used for optimising drug properties, it is critical to establish that they can produce quantitative pharmacological feedback when comparing related drugs (*Hopkins, 2008*).

Aggregated IR-DR assay score directly relates to pharmacologically derived in vitro potency

The relationship between in vitro drug potency and IR-DR assay score for 37 compounds (*Appendix 1—figure 5*), nominally targeting epidermal growth factor receptor (EGFR or HER1) tyrosine kinase, was investigated. This stress-induced inflammatory protein has recently emerged as a target for treating metabolic disease and neurodegeneration (*Donath, 2021*; *Menden et al., 2019*; *Norambuena et al., 2017*). One endogenous EGFR ligand, amphiregulin, is induced by high-fat feeding to drive TNF-mediated IR (*Skurski et al., 2020*), while EGFR is overexpressed in astrocytes of Alzheimer's disease (AD). The EGFR inhibitor afatinib (IR-DR score = 77) attenuates astrocyte activation (*Chen et al., 2019*) while inhibition of EGFR can reduce FOXK1 and FOXK2 phosphorylation (*Klaeger et al., 2017*) to normalise mTORC1-regulated autophagy and reduce IR (*Bowman et al., 2014*; *Jahng et al., 2019*). Nine EGFR inhibitors have been screened against >300 kinases (*Davis et al., 2011*; *Klaeger et al., 2017*), which enabled us to directly contrast laboratory-derived kinase selectivity with the IR-DR score. Potency versus EGFR directly related to IR-DR assay score (*Figure 3A*), yet this could not fully explain why certain compounds were inactive. Cluster analysis of the most targeted proteins (<300 nM potency for at least one compound) illustrated that alisertib, the only potent EGFR inhibitor with a negative IR-DR score (–90), inhibited PLK4, AURKB and AURKA (*Figure 3B*). Orantinib, a 24 nM inhibitor of AURKB, also had a negative IR-DR score (–77), as did MK-5108, an inhibitor of AURKB and AURKA (–90), indicating that alisertib's profile reflects pharmacology beyond EGFR (probably AURKB as AURKB KD had an IR-DR score of –83, Table S3).

Multiple protein targets help explain the positive activity of EGFR targeting drugs

A broader exploration of 'EGFR' inhibitor targets provides a better understanding of the activity of this group of compounds in the IR-DR assay. For example, neutral scoring bosutinib and neratinib target several mitogen-activated protein kinase (MAPK) family members, and some of these oppose positive IR-DR scoring, for example, MAP2K2 (–78, Table S4). Neutral scoring, yet potent EGFR inhibitors (e.g. neratinib, bosutinib and lapatinib) also inhibit the related proteins, ERBB2, ERBB3 and ERBB4 (<5 nM, HER2-4). Some of these family members may represent beneficial 'off targets' while others may be detrimental (*Moret et al., 2019*). For example, hyperglycaemia induces erbb4 in mice and erbb4 expression is increased in AD (*Huh et al., 2016*; *Woo et al., 2011*), where OE increases tau phosphorylation via mTOR activation (*Nie et al., 2018b*). Gefitinib (an EGFR inhibitor) reduces IR-mediated glucose excursions in vivo in a RIPK2-dependent manner (*Duggan et al., 2020*) and rescues memory deficits in mice at a very low chronic dose of 0.01 mg/kg (*Wang et al., 2012*). Loss of RIPK2 (or a dominant-negative mutant of RIPK2) prevents excessive NFκB activation (*Chin et al., 2002*), and RIPK2 is a downstream effector of innate immunity (TLR signalling).

Some EGFR targeting drugs also potently inhibit the tyrosine kinase ABL1, and loss of adipose ABL1 reduces obesity-induced IR in the mouse (*Wu et al., 2017*). Erlotinib (IR-DR score = +72), which also inhibits ABL1, reduces kidney inflammation and preserves pancreas function and insulin sensitivity in a mouse model of diabetes (*Li et al., 2018b*). Furthermore, Aβ activates neuronal ABL1 in vitro, intra-hippocampal injection of Aβ fibrils increases expression of ABL1 in vivo and imatinib (STI571), a 90 nM inhibitor of ABL1, inhibits ABL1-mediated Aβ neurodegenerative pathways (*Cancino et al., 2011*; *Cancino et al., 2008*; *Gutierrez et al., 2019*). However, imatinib does not yield a significant IR-DR score (nor inhibit EGFR), indicating that targeting ABL1 alone might be insufficient to treat human IR. Importantly, potency of the EGFR inhibitors against ABL1 also correlates with their potency against several ephrin receptors (EPHA5 R = 0.74, EPHA6 R = 0.95 and EPHA8 R = 0.76), as well as with RIPK2 (R = 0.77). Oral dosing of the ephrin A receptor inhibitor, UniPR500, reverses high-fat feeding-induced glucose intolerance without changes in plasma insulin (*Giorgio et al., 2019*), and these benefits likely reflect UniPR500 targeting proteins in common with our top-ranked 'EGFR' kinase inhibitors. Thus, while drug potency against EGFR quantitatively tracks with the IR-DR score (*Figure 3A*), this may reflect binding affinity at other related protein kinases, and identification of these additional targets is important (*Redhead et al., 2021*).
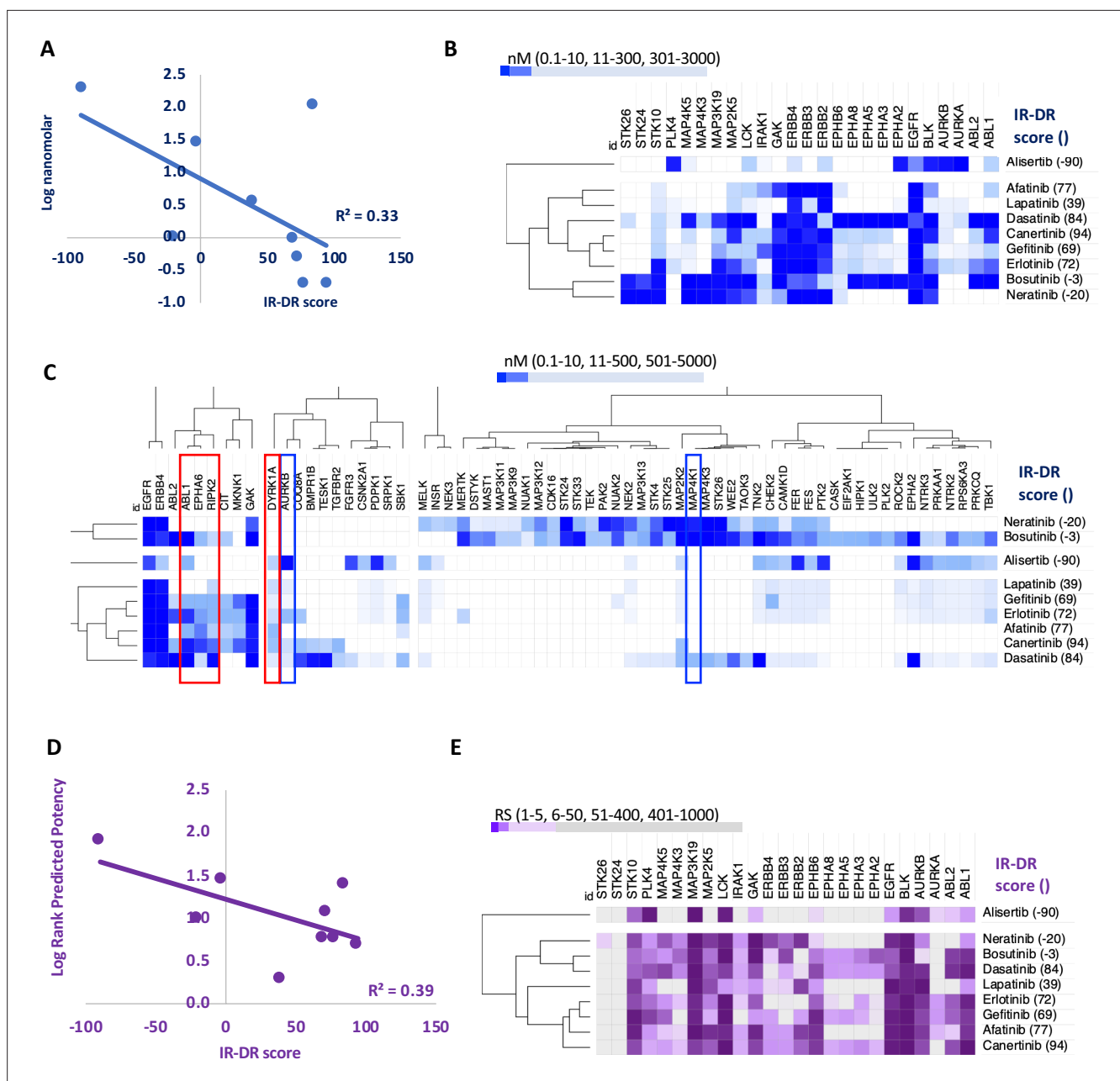
Figure 3. An analysis of the relationship between the insulin resistance-drug repurposing (IR-DR) score and laboratory-based pharmacological potency and selectivity or deep learning-based predictions of compound potency and selectivity. (**A**) Inhibitory constants (nM) derived from laboratory assays against top-ranked targets for a series of epidermal growth factor receptor (EGFR) inhibitors. (**B**) Relationship between IR-DR score (100 = best score) and log potency against EGFR. (**C**) Expanded range of known targets, for at least one of the inhibitors, helps identify potentially positive (red box) and negative (blue box) off-target inhibitory actions. (**D**) Rank order score (RS, 1–19211) of predicted compound binding for all protein-coding genes using the DeepPurpose ML model; lab-validated targets feature in top 0.15% of target predictions. Log rank order ('predicted potency') for EGFR, over the protein-coding genome, partly predicts efficacy in IR-DR assay, confirming that the ML model matches the relationship observed using the laboratory pharmacology. (**E**) Using the predicted protein targets and the DeepPurpose rank order scores, it is possible to cluster positively acting 'EGFR' compounds from less active or negatively acting compounds.

A DL model of genome-wide binding affinity ranks compound affinity in the IR-DR assay

Thus we find that (*Figure 3A–C*) the best scoring potent 'EGFR' kinase inhibitors reflect a balance of activities against positively and negatively acting *kinases* and that this is partly interpretable versus the extensive in vitro screening data for those drugs (*Davis et al., 2011*; *Klaeger et al., 2017*).

Genome-wide pharmacological profiles are however prohibitively costly and thus often unavailable. Predicted drug-protein interactions, using emerging techniques from graph machine learning (*Sturm et al., 2020*), aim to overcome this lack of laboratory data. Using the DeepPurpose DL suite of algorithms (*Huang et al., 2021*), we modelled EGFR family kinase inhibitors as simplified molecular-input line-entry system (SMILES) string and all proteins by their amino acid sequence (a strategy that obfuscates the need for 3D structures obtained by costly experimental models). This expanded the scope of drug target information of the EGFR inhibitors discussed above to a genome-wide level (Tables S6-S8). Each of the EGFR inhibitors was scored against 19,211 proteins using 14 pre-trained models (Table S9), and we relied on a fusion of ranking scores across models to identify the top protein targets of each compound.

The nine EGFR inhibitors described above inhibit 25 proteins with nanomolar potency (<300 nM), and the DL model accurately ranked these proteins in the top 0.1–1.7% of all 2,420,586 predictions (median = 0.15%, Table S6). The DL-predicted rank score ('potency') against EGFR strongly related to the measured IR-DR score (*Figure 3D*), replicating the potency-activity relationship noted using laboratory data (*Figure 3A*) correctly clustering the nine compounds (*Figure 3C*, *Appendix 1—figure 9A*). DL also ranked several proteins that we already identified may compromise a positive IR-DR score (*Figure 3E*, *Appendix 1—figure 9*). For example, AURKB was a top-ranked predicted target for alisertib (26/19211), aligning with the data that inhibition of AURKB drives a negative IR-DR score. Additional predicted protein targets (Table S8) will also influence the IR-DR score, independently of EGFR, for example, MERTK, KCNH6 and PTK2B (*Appendix 1—figure 9*). Loss of PTK2B (focal adhesion kinase 2 [FAK2]), a risk gene for the development of tauopathy in AD (*Tan et al., 2021*), can promote the development of IR in vivo and in adipocytes (*Luk et al., 2017*; *Yu et al., 2005*) while inhibition of KCNH6 should probably be avoided,as it regulates insulin secretion (*Yang et al., 2018*). In contrast, a genetic loss-of-function variation in MERTK appears protective against IR, fatty liver disease and pro-inflammatory mediators in humans (*Musso et al., 2017*), and thus it represents a potential protein target against which current 'EGFR' inhibitors should be screened against. Therefore, we applied the same modelling strategy to 16 of the 28 less well-characterised EGFR inhibitors with proven sub-micromolar activity. Each was ranked highly by the model against EGFR (Table S7)**,** with MAP3K19 being one of the highest ranked additional targets (*Appendix 1—figure 10*)**,** and there was a negative correlation between predicted MAP3K19 binding and IR-DR score (*Appendix 1—figure 10*). Little is known about MAP3K19 (a 'dark' kinase) other than that it may contribute to ERK pathway activation (*Hoang et al., 2020*) – and some ERK inhibitors proved positive scoring in the IR-DR assay (*Appendix 1—figure 3*) – and thus MAP3K19 may be a novel positive effector of insulin signalling. MAP3K19 is not abundantly expressed in adipose or muscle tissue (lowest 10th percentile of gene expression in our studies) such that net compound efficacy in vivo may also reflect tissue-specific patterns of protein activity.

General conclusions and limitations

We illustrate that a cell-line transcriptome-based high-throughput DR assay yields interpretable and quantitative pharmacological data when designed around robust clinical RNA signatures, and that DL-based drug target predictions can be used to interpret assay scores. Some of the drugs we identified may be suitable for treating acute IR, such as occurring during infection (*Ceriello et al., 2020*; *Donath, 2021*), and encouragingly several positive scoring drugs appear tolerable in longer-term preclinical models of metabolic or neurogenerative disease (*Li et al., 2018b*; *Wang et al., 2012*). The present approach could be extended to include a stratified medicine component, where evaluation of positively acting compounds is first trialled in T2DM patients with extreme IR (*Choi et al., 2019*). A number of positively acting IR-DR compounds, including selected mTOR inhibitors (*Appendix 1—figure 3*), are able to mimic a longevity-related RNA signature (*Timmons et al., 2019*) and thus may be potential geroprotectors (*Fuentealba et al., 2019*). A more extensive multi-disease signature approach could ultimately help tailor the DR process to the individual patient. We do acknowledge that some IR-DR assay negative scores may be false negatives, for example, selective HDAC inhibition (HDACi) can, through lower and shorter daily exposure (*Sartor et al., 2019*; *Volmar et al., 2017*), be beneficial (although positive attributes of HDACi on IR appear to reflect non-specific actions; *Martins et al., 2019*). Furthermore, despite correctly matching with nuclear receptor-induced muscle transcriptome signatures in vivo, there was a dearth of matches in vitro indicating that further optimisation

of the IR-DR assay format is merited. It can be the case that certain classes of ligand require more sophisticated assay condition or require the use of primary cells. In conclusion; human transcriptome signatures, classic pharmacological assays, drug action in vivo and DL-based target prediction consistently link with drug transcriptional profiles in cell lines, establishing that expansion of such resources represents an important strategy for future DR efforts.

Materials and methods

Key resources table

Reagent type (species) or resource	Designation	Source or reference	Identifiers	Additional information
Software, algorithm	R	https://www.r-project.org/	3.6.3 and 4.04	
Software, algorithm	Python	https://www.python.org/	D1306	
Software, algorithm	DeepPurpose	https://github.com/kexinhuang12345/DeepPurpose.git; *Huang et al., 2021*	2020	
Software, algorithm	Venny	https://bioinfogp.cnb.csic.es/tools/venny/	2.10	
Software, algorithm	Metascape	http://metascape.org/gp/index.html#/main/step1	2020	
Software, algorithm	CLUE	https://clue.io/	March 2020	
Software, algorithm	PubChem	https://pubchem.ncbi.nlm.nih.gov/	December 2020	
Software, algorithm	PubMed	https://pubmed.ncbi.nlm.nih.gov/	December 2020	
Software, algorithm	SMS	https://labsyspharm.shinyapps.io/smallmoleculesuite/	December 2020	
Software, algorithm	iLINCS	http://www.ilincs.org/ilincs/signatures/search/	March 2020	
Software, algorithm	Morpheus	https://clue.io/morpheus	2021	
Software, algorithm	Code	Source_code_file.docx	-	R/Python code used in project

We utilised human muscle and adipose tissue transcriptome profiles from multiple large studies (*Civelek et al., 2017*; *Nakhuda et al., 2016*; *Slentz et al., 2016*; *Timmons et al., 2018*). The individual sample identifiers utilised in this study are reported (*Appendix 1—figure 10*) and deposited online at GEO. Gene expression (IRON-normalised data; *Welsh et al., 2013*) was contrasted against log-transformed HOMA2-IR values (measured in fasting blood [*Wallace et al., 2004*] using the Excel-based version of http://www.dtu.ox.ac.uk/homacalculator, adjusting for patient age) using ANOVA and linear regression (*Timmons et al., 2018*). A robust transcriptional signature of IR shared across two human insulin-targeted tissues was identified (from a total of 337 genes significantly regulated in muscle, FDR < 5%, absolute correlation-coefficient (CC) >0.15); this represented our 'disease signature' (*Appendix 1—figure 11*). Gene expression responses that are proportional to treatment efficacy (reduced IR) and consistent across two human tissue types have not been previously investigated. Change in gene expression was derived from biopsy samples obtained before and following supervised lifestyle intervention. Lifestyle intervention ranged from aerobic to resistance training with modest calorie restriction, and varied in duration from 15 min (e.g. high-intensity cycle-based exercise) to >1 hr 3 days a week, as previously detailed (*AbouAssi et al., 2015*; *Nakhuda et al., 2016*; *Phillips et al., 2017*; *Slentz et al., 2011*). In short, we located genes tracking with efficacy, regardless of clinical protocol or 'dosage'. Change in gene expression was related to change in HOMA2-IR identifying a consistent 'treatment signature' for muscle (mean q-value < 0.08, CC values consistent in 3/4 of muscle studies), and then those similarly regulated in adipose tissue were retained.

Feature selection and in vivo DR validation step

The disease and the treatment genes lists represent the pool of features from which we selected IR-DR signatures. Quantitative network modelling (*Song and Zhang, 2015*) was applied to tissue expression values of these genes, as previously described (*Timmons et al., 2019*), to identify hub genes; genes with greater connectivity (*Appendix 1—figure 1*). Four alternative similarly sized sets of genes were selected for validation, comprising 60 positively associated and 60 negatively associated RNAs. The final models shared only two genes named as candidates from genome-wide IR association studies (*Lotta et al., 2017*), and those genes (INSR and GRB14) were not essential for our analysis. To rank the performance of each of our four RNA assays (Table S1), we utilised DrugMatrix, a database of in vivo rodent tissue drug-response signatures (http://www.ilincs.org/ilincs/) that includes TZD and oestrogen-related molecules known to reverse IR in vivo (*Hevener et al., 2018*; *Sears et al., 2009*) and target IR pathways in cell models (*Sood et al., 2016*). Signatures validated at this stage were considered suitable for further use. Lists that failed this step (lists 4 and 5) included genes inferred from genome-wide IR association studies, and T2DM proteome biomarkers (*Gudmundsdottir et al., 2020*; *Lotta et al., 2017*; *Vujkovic et al., 2020*) were modelled in vitro only to produce summary statistics for Table S1.

In vitro DR analysis

The in vivo-validated IR signatures were screened using the largest public database of in vitro drug signatures (*Subramanian et al., 2017*) via the clue.io resource (version 1, 2020). These drug transcriptional signatures were generated in nine cell lines, and while each cell line captures some unique signals from each compound (*Baillif et al., 2020*), part of this will be noise, reflecting the small sample size (typically n = 3). Therefore, we used aggregated signature matching across the nine human cell lines (PC3, VCAP, A375, A549, HA1E, HCC515, HT29, MCF7 and HEPG2) to both deliberately reduce the influence of cell line-specific effects (*Xu et al., 2018*) and to increase the sample size ninefold (*Subramanian et al., 2017*). Active compounds were those with scores exceeding ~10th percentile of positive and negative scores (*Appendix 1—figure 3*), a value that represents the mean threshold (±1 standard deviation) of scores exceeding the assay scoring threshold (*Subramanian et al., 2017*). The use of aggregated scores across cell types was validated using an extensive validation process (*Figure 1*). In addition to our IR-DR assay, we considered two additional in vivo RNA models. One is a novel 141-gene human-derived muscle growth signature (*Stokes et al., 2020*), which demonstrated – as expected – that the clue.io database contains a sizeable number of compounds known to inhibit cell growth (negative-scoring compounds, *Appendix 1—figure 2* and *Appendix 1—figure 3*). The second was an IR-adjusted longevity-associated signature (*Timmons et al., 2019*), which identified relevant drug matches from the cell-line perturbagen database (*Appendix 1—figure 2* and 'Discussion'). The output from each assay was a list of >2500 DR scores, each assigned to a particular assay ID and drug name. There then followed a laborious manual annotation process, reflecting that study of drugs is challenging (*Christmann-Franck et al., 2016*), and annotation errors populate all databases, including iLINCS. For all of the active compounds, we carried out a manual check to ensure that compound labels in CLUE were verifiable in Chembl (*Mendez et al., 2019*), and that both were consistent with the data deposited in the small molecule suit (*Moret et al., 2019*). The manually confirmed data progressed to the next phase of the analysis.

Characterisation of active compounds

Active compounds belonged to a wide range of distinct pharmacological classes (*Appendix 1—figures 4 and 5*). To identify if positive and negatively acting compounds (from IR-DR score) could be easily distinguished from each other, we calculated simple molecular descriptors. A set of 2837 compounds for which in vitro results were available was considered, and chemical structures were extracted from the CLUE database (https://clue.io/) as SMILES strings. These were parsed with RDKit (version 2020.03.6), with 14 compounds failing to parse correctly. For each compound, a set of 13 physicochemical descriptors was calculated with RDKit including molecular weight, heavy atom count, number of heteroatoms, LogP, number of rotatable bonds, topological polar surface area (TPSA), number of rings, number of aromatic rings, number of saturated rings, number of aliphatic rings, Balaban's J index, number of hydrogen bond donors and number of hydrogen bond acceptors. Positive acting compounds were coloured in orange, and negative acting in blue (*Appendix 1—figure 6*). For

each compound active against list 3A IR-DR signature (*Appendix 1—figure 3*), we identified their protein targets using a variety of resources (*Christmann-Franck et al., 2016*, https://www.ebi.ac.uk/chembl/, https://clue.io/, and https://pubchem.ncbi.nlm.nih.gov/). The small-molecule suite was used to extract laboratory-derived potency values against each protein (https://labsyspharm.shinyapps.io/smallmoleculesuite/). Very few compounds are profiled against the majority (>300 kinases. For those that had values, in vitro potency values (log10) were plotted against the IR-DR scores and Pearson's correlation coefficients calculated in Excel, allowing us to establish the relationship between potency against a protein and the IR-DR score. Very extensive manual PubMed searches were then undertaken to characterise the positive and negative acting drugs using the terms 'drug name' 'alternative drug name' with the following terms used in sequence until either relevant publications were identified or no hits were obtained; insulin, diabetes, obesity, dementia, Alzheimer's disease, COVID-19 and inflammation (during 2020).

Single-gene manipulation and network biology

The in vitro drug signatures in clue.io are the most robust data from that project (*Subramanian et al., 2017*). However, the database also contains gene KD (n = 3799 genes) and OE (n = 2161 genes) data, making it possible to link the IR-DR signature with specific protein targets. The KD or OE activity score was again averaged across 6–9 cell lines, and we considered protein targets derived from the known targets of the active compound list (to limit the known higher false-positive rate with the KD/OE data; *Subramanian et al., 2017*). As stated in the results, >15% of IR-active drug targets yielded a significant IR-DR score. In comparison, a total of 459 genes were associated with an IR-DR score at a threshold of >70 or <-70, representing 265 positive associations (mean = 85) and 194 negative IR-DR scores (mean = –83), equalling only ~7% of all 5954 genomic assays. The pathway biology of the 73 independently validated protein targets was analysed using Metascape (*Zhou et al., 2019*), along with the IR-DR signature (*Table 1*, *Appendix 1—figure 2*), where 'Combo_sig' represents the IR-DR pathways, and the 73 genes split into two lists depending on how KD or OE impacted on the IR-DR signature match (Table S4). For the data plot, edges represent connected GO biological processes (>0.3), and nodes within each cluster are coloured/named by their most statistically enriched GO term (*Figure 3B*). Each node is presented as a pie chart, scaled in size by the total number of terms represented by that (top-scoring) ontology, and with the 'slices' coloured to indicate from which gene list the terms originate. The network structure is separately colour-coded (*Figure 3C*) by list membership to identify when drugs directly target IR-DR assay pathways (red); when KD or OE genes negatively correlated (blue) with the IR-DR score (inhibition yields a positive or OE yields a negative IR-DR score) or positively correlated (green) with the IR-DR score.

Drug-target interaction prediction with DeepPurpose

To investigate the mechanisms of action of positively acting IR-DR compounds, we extended the existing pharmacological data with computationally derived drug-target interaction (DTI) predictions. Publicly available chemogenomic databases are very far from complete, and therefore, ML modelling approaches can be used to provide estimates for missing data. DL-based models have shown promise in this context (*Gaudelet et al., 2021*; *James et al., 2020*). We used DeepPurpose, a DL library for DTI prediction (*Huang et al., 2021*) that takes as an input SMILES of the small molecules of interest and the amino acid sequences of the protein-coding genome. Different encoders were implemented to provide a compound and a protein embedding. The small molecule and protein embeddings are concatenated and fed to a multi-layer perceptron that predicts the binding affinity as a dissociation constant (K_d). DeepPurpose provides a set of pre-trained models that can be used 'off-the-shelf'. We used 14 pre-trained models that were available as of 01/12/2020. Those models differ from one another depending on the encoders and on the DTI training set. Drug encoders included convolutional neural network (CNN), daylight fingerprints, Morgan fingerprints and message-passing neural network (MPNN), while protein encoders amino acid composition (AAC) and CNN were used. The training sets were BindingDB (*Liu et al., 2007*), DAVIS (*Davis et al., 2011*) and KIBA (*Tang et al., 2014*). A list of the models used is shown in Table S9. All DTI models described above were applied to obtain 14 rankings of 19,211 human proteins as potential

targets for each compound. A final score was obtained by an average ranking of each protein across 14 models, with the final top-ranking targets predicted to be the most likely protein targets of the input drug list. Comparable consensus-oriented strategies are often applied in virtual screening to exploit the strengths of multiple models (*Gaudelet et al., 2021*; *James et al., 2020*) and achieve improved performance (*Palacio-Rodríguez et al., 2019*; *Perez-Castillo et al., 2017*). DeepPurpose models showed promising performance in various testing scenarios, and we refer to the original publication for further details. The code used for the entire analysis can be located in the supplemental document.

Acknowledgements

Additional information

Competing interests

James A Timmons: received consultancy fees from McMaster University, and has a majority share of the stock in Augur Precision Medicine LTD. A patent may be processed for the drug screen. Andrew Anighoro, Jake Taylor-King: is an employee of Relation Therapeutics LTD and owns stocks in the company. The author has no other competing interests to declare. Robert J Brogan: is affiliated with Augur Precision Medicine LTD. An application for the drug signature may be processed by the lead parties in the project. Jack Stahl, Claes Wahlestedt, Claude-Henry Volmar: An application for the drug signature may be processed by the lead parties in the project. David Gordon Farquhar: is affiliated with Augur Precision Medicine LTD and owns stocks in the company. An application for the drug signature may be processed by the lead parties in the project. Stuart M Phillips: received travel fees and honoraria from the US National Dairy Council and the US Dairy Export Council. SP also received fees from Enhanced Recovery which were donated to charity. SP has a Canadian patent issued (Canadian patent 3052324 issued to Exerkine) and a US patent pending US patent 16/182891 pending to Exerkine, with no financial gains associated with these patents. The author has no other competing interests to declare. The other author declares that no competing interests exist.

Funding

Funder	Grant reference number	Author
Natural Sciences and Engineering Research Council of Canada	RGPIN-2020	Stuart M Phillips
National Institute on Aging	R56AG061911	Claude-Henry Volmar James Timmons Claes Wahlestedt
Queen Mary University London	BHF Senior Fellowship	James A Timmons

The funders had no role in study design, data collection and interpretation, or the decision to submit the work for publication.

Author contributions
James A Timmons, Conceptualization, Formal analysis, Funding acquisition, Investigation, Project administration, Resources, Supervision, Visualization, Writing – original draft, Writing – review and editing, Data curation, Methodology; Andrew Anighoro, Formal analysis, Investigation, Methodology, Writing – original draft, Writing – review and editing; Robert J Brogan, Data curation, Writing – review and editing, Formal analysis, Validation; Jack Stahl, Data curation, Writing – review and editing; Claes Wahlestedt, Claude-Henry Volmar, Supervision, Writing – review and editing; David Gordon Farquhar, Funding acquisition, Project administration, Resources, Writing – review and editing; Jake Taylor-King, Conceptualization, Supervision, Writing – review and editing; William E Kraus, Funding acquisition, Resources, Writing – review and editing; Stuart M Phillips, Conceptualization, Data curation, Funding acquisition, Investigation, Resources, Writing – original draft

Author ORCIDs
James A Timmons http://orcid.org/0000-0002-2255-1220
Claude-Henry Volmar http://orcid.org/0000-0001-9437-051X
William E Kraus http://orcid.org/0000-0003-1930-9684
Stuart M Phillips http://orcid.org/0000-0002-1956-4098

Decision letter and Author response
Decision letter https://doi.org/10.7554/eLife.68832.sa1
Author response https://doi.org/10.7554/eLife.68832.sa2

Additional files

Supplementary files
- Transparent reporting form
- Supplementary file 1. Supplementary Tables 1–10.
- Source code 1. Computational code used in the present study.

Data availability
The gene expression data sets are available at GSE154846, GSE58559 and GSE70353.

The following previously published datasets were used:

Author(s)	Year	Dataset title	Dataset URL	Database and Identifier
Timmons JA	2018	META-PREDICT: Dynamic responses of the global human skeletal muscle coding and noncoding transcriptome to exercise	https://www.ncbi.nlm.nih.gov/geo/query/acc.cgi?acc=GSE154846	NCBI Gene Expression Omnibus, GSE154846
Civelek M	2017	Subcutaneous adipose tissue gene expression from men that are part of the METSIM study	https://www.ncbi.nlm.nih.gov/geo/query/acc.cgi?acc=GSE70353	NCBI Gene Expression Omnibus, GSE70353
Josse AR, Timmons JA	2016	Human adipose tissue profiled before and after 16 weeks of intense exercise training with a modest energy deficit	https://www.ncbi.nlm.nih.gov/geo/query/acc.cgi?acc=GSE58559	NCBI Gene Expression Omnibus, GSE58559

References

AbouAssi H, Slentz CA, Mikus CR, Tanner CJ, Bateman LA, Willis LH, Shields AT, Piner LW, Penry LE, Kraus EA, Huffman KM, Bales CW, Houmard JA, Kraus WE. 2015. The effects of aerobic, resistance, and combination training on insulin sensitivity and secretion in overweight adults from STRRIDE AT/RT: a randomized trial. *Journal of Applied Physiology* 118:1474–1482. DOI: https://doi.org/10.1152/japplphysiol.00509.2014, PMID: 25882384

Aerts JM, Ottenhoff R, Powlson AS, Grefhorst A, van Eijk M, Dubbelhuis PF, Aten J, Kuipers F, Serlie MJ, Wennekes T, Sethi JK, O'Rahilly S, Overkleeft HS. 2007. Pharmacological inhibition of glucosylceramide

synthase enhances insulin sensitivity. *Diabetes* **56**:1341–1349. DOI: https://doi.org/10.2337/db06-1619, PMID: 17287460

Alfazema N, Barrier M, de Procé SM, Menzies RI, Carter R, Stewart K, Diaz AG, Moyon B, Webster Z, Bellamy COC, Arends MJ, Stimson RH, Morton NM, Aitman TJ, Coan PM. 2019. Camk2n1 Is a Negative Regulator of Blood Pressure, Left Ventricular Mass, Insulin Sensitivity, and Promotes Adiposity. *Hypertension* **74**:687–696. DOI: https://doi.org/10.1161/HYPERTENSIONAHA.118.12409, PMID: 31327268

Amamoto T, Kumai T, Nakaya S, Matsumoto N, Tsuzuki Y, Kobayashi S. 2006. The elucidation of the mechanism of weight gain and glucose tolerance abnormalities induced by chlorpromazine. *Journal of Pharmacological Sciences* **102**:213–219. DOI: https://doi.org/10.1254/jphs.fp0060673, PMID: 17031068

Baillif B, Wichard J, Méndez-Lucio O, Rouquié D. 2020. Exploring the Use of Compound-Induced Transcriptomic Data Generated From Cell Lines to Predict Compound Activity Toward Molecular Targets. *Frontiers in Chemistry* **8**:296. DOI: https://doi.org/10.3389/fchem.2020.00296, PMID: 32391323

Blagosklonny MV. 2017. From rapalogs to anti-aging formula. *Oncotarget* **8**:35492–35507. DOI: https://doi.org/10.18632/oncotarget.18033, PMID: 28548953

Bowman CJ, Ayer DE, Dynlacht BD. 2014. Foxk proteins repress the initiation of starvation-induced atrophy and autophagy programs. *Nature Cell Biology* **16**:1202–1214. DOI: https://doi.org/10.1038/ncb3062, PMID: 25402684

Brown AS, Patel CJ. 2018. A review of validation strategies for computational drug repositioning. *Briefings in Bioinformatics* **19**:174–177. DOI: https://doi.org/10.1093/bib/bbw110, PMID: 27881429

Budi EH, Hoffman S, Gao S, Zhang YE, Derynck R. 2019. Integration of TGF-β-induced Smad signaling in the insulin-induced transcriptional response in endothelial cells. *Scientific Reports* **9**:1–16. DOI: https://doi.org/10.1038/s41598-019-53490-x, PMID: 31740700

Cancino GI, Toledo EM, Leal NR, Hernandez DE, Yévenes LF, Inestrosa NC, Alvarez AR. 2008. STI571 prevents apoptosis, tau phosphorylation and behavioural impairments induced by Alzheimer's beta-amyloid deposits. *Brain : A Journal of Neurology* **131**:2425–2442. DOI: https://doi.org/10.1093/brain/awn125, PMID: 18559370

Cancino GI, Perez de Arce K, Castro PU, Toledo EM, von Bernhardi R, Alvarez AR. 2011. c-Abl tyrosine kinase modulates tau pathology and Cdk5 phosphorylation in AD transgenic mice. *Neurobiology of Aging* **32**:1249–1261. DOI: https://doi.org/10.1016/j.neurobiolaging.2009.07.007, PMID: 19700222

Ceriello A, Standl E, Catrinoiu D, Itzhak B, Lalic NM, Rahelic D, Schnell O, Škrha J, Valensi P, Diabetes and Cardiovascular Disease (D&CVD) EASD Study Group. 2020. Issues of Cardiovascular Risk Management in People With Diabetes in the COVID-19 Era. *Diabetes Care* **43**:1427–1432. DOI: https://doi.org/10.2337/dc20-0941, PMID: 32409501

Chakraborti AK, Garg SK, Kumar R, Motiwala HF, Jadhavar PS. 2010. Progress in COX-2 inhibitors: a journey so far. *Current Medicinal Chemistry* **17**:1563–1593. DOI: https://doi.org/10.2174/092986710790979980, PMID: 20166930

Chan PC, Wu TN, Chen YC, Lu CH, Wabitsch M, Tian YF, Hsieh PS. 2018. Targetted inhibition of CD74 attenuates adipose COX-2-MIF-mediated M1 macrophage polarization and retards obesity-related adipose tissue inflammation and insulin resistance. *Clinical Science* **132**:1581–1596. DOI: https://doi.org/10.1042/CS20180041, PMID: 29773671

Chen YJ, Hsu CC, Shiao YJ, Wang HT, Lo YL, Lin AMY. 2019. Anti-inflammatory effect of afatinib (an EGFR-TKI) on OGD-induced neuroinflammation. *Scientific Reports* **9**:1–10. DOI: https://doi.org/10.1038/s41598-019-38676-7, PMID: 30792526

Chen H, Cheng F, Li J. 2020. iDrug: Integration of drug repositioning and drug-target prediction via cross-network embedding. *PLOS Computational Biology* **16**:e1008040. DOI: https://doi.org/10.1371/journal.pcbi.1008040, PMID: 32667925

Cheng F, Liu C, Jiang J, Lu W, Li W, Liu G, Zhou W, Huang J, Tang Y. 2012. Prediction of drug-target interactions and drug repositioning via network-based inference. *PLOS Computational Biology* **8**:e1002503. DOI: https://doi.org/10.1371/journal.pcbi.1002503, PMID: 22589709

Chin AI, Dempsey PW, Bruhn K, Miller JF, Xu Y, Cheng G. 2002. Involvement of receptor-interacting protein 2 in innate and adaptive immune responses. *Nature* **416**:190–194. DOI: https://doi.org/10.1038/416190a, PMID: 11894097

Chiu HY, Chiang CM, Yeh SP, Jong DS, Wu LS, Liu HC, Chiu CH. 2020. Effects of hyperinsulinemia on acquired resistance to epidermal growth factor receptor-tyrosine kinase inhibitor via the PI3K/AKT pathway in non-small cell lung cancer cells in vitro. *Oncology Letters* **20**:206. DOI: https://doi.org/10.3892/ol.2020.12069, PMID: 32963612

Choi SE, Berkowitz SA, Yudkin JS, Naci H, Basu S. 2019. Personalizing Second-Line Type 2 Diabetes Treatment Selection: Combining Network Meta-analysis, Individualized Risk, and Patient Preferences for Unified Decision Support. *Medical Decision Making* **39**:239–252. DOI: https://doi.org/10.1177/0272989X19829735, PMID: 30767632

Christmann-Franck S, van Westen GJP, Papadatos G, Beltran Escudie F, Roberts A, Overington JP, Domine D. 2016. Unprecedently Large-Scale Kinase Inhibitor Set Enabling the Accurate Prediction of Compound-Kinase Activities: A Way toward Selective Promiscuity by Design? *Journal of Chemical Information and Modeling* **56**:1654–1675. DOI: https://doi.org/10.1021/acs.jcim.6b00122, PMID: 27482722

Civelek M, Wu Y, Pan C, Raulerson CK, Ko A, He A, Tilford C, Saleem NK, Stančáková A, Scott LJ, Fuchsberger C, Stringham HM, Jackson AU, Narisu N, Chines PS, Small KS, Kuusisto J, Parks BW, Pajukanta P, Kirchgessner T, et al. 2017. Genetic Regulation of Adipose Gene Expression and Cardio-Metabolic Traits.

American Journal of Human Genetics **100**:428–443. DOI: https://doi.org/10.1016/j.ajhg.2017.01.027, PMID: 28257690

Copps KD, Hançer NJ, Qiu W, White MF. 2016. Serine 302 Phosphorylation of Mouse Insulin Receptor Substrate 1 (IRS1) Is Dispensable for Normal Insulin Signaling and Feedback Regulation by Hepatic S6 Kinase. *The Journal of Biological Chemistry* **291**:8602–8617. DOI: https://doi.org/10.1074/jbc.M116.714915, PMID: 26846849

Davis MI, Hunt JP, Herrgard S, Ciceri P, Wodicka LM, Pallares G, Hocker M, Treiber DK, Zarrinkar PP. 2011. Comprehensive analysis of kinase inhibitor selectivity. *Nature Biotechnology* **29**:1046–1051. DOI: https://doi.org/10.1038/nbt.1990, PMID: 22037378

Donath MY. 2021. Glucose or Insulin, Which Is the Culprit in Patients with COVID-19 and Diabetes? *Cell Metabolism* **33**:2–4. DOI: https://doi.org/10.1016/j.cmet.2020.11.015, PMID: 33248018

Duggan BM, Cavallari JF, Foley KP, Barra NG, Schertzer JD. 2020. RIPK2 Dictates Insulin Responses to Tyrosine Kinase Inhibitors in Obese Male Mice. *Endocrinology* **161**:bqaa086. DOI: https://doi.org/10.1210/endocr/bqaa086, PMID: 32473019

Everett BM, Donath MY, Pradhan AD, Thuren T, Pais P, Nicolau JC, Glynn RJ, Libby P, Ridker PM. 2018. Anti-Inflammatory Therapy With Canakinumab for the Prevention and Management of Diabetes. *Journal of the American College of Cardiology* **71**:2392–2401. DOI: https://doi.org/10.1016/j.jacc.2018.03.002, PMID: 29544870

Fiore D, Gianfrilli D, Giannetta E, Galea N, Panio G, di Dato C, Pofi R, Pozza C, Sbardella E, Carbone I, Naro F, Lenzi A, Venneri MA, Isidori AM. 2016. PDE5 Inhibition Ameliorates Visceral Adiposity Targeting the miR-22/SIRT1 Pathway: Evidence From the CECSID Trial. *The Journal of Clinical Endocrinology and Metabolism* **101**:1525–1534. DOI: https://doi.org/10.1210/jc.2015-4252, PMID: 26964730

Fiore D, Gianfrilli D, Cardarelli S, Naro F, Lenzi A, Isidori AM, Venneri MA. 2018. Chronic phosphodiesterase type 5 inhibition has beneficial effects on subcutaneous adipose tissue plasticity in type 2 diabetic mice. *Journal of Cellular Physiology* **233**:8411–8417. DOI: https://doi.org/10.1002/jcp.26796, PMID: 29797572

Fontaine J, Tavernier G, Morin N, Carpéné C. 2020. Vanadium-dependent activation of glucose transport in adipocytes by catecholamines is not mediated via adrenoceptor stimulation or monoamine oxidase activity. *World Journal of Diabetes* **11**:622–643. DOI: https://doi.org/10.4239/wjd.v11.i12.622, PMID: 33384769

Fowler AJ, Hebron M, Balaraman K, Shi W, Missner AA, Greenzaid JD, Chiu TL, Ullman C, Weatherdon E, Duka V, Torres-Yaghi Y, Pagan FL, Liu X, Ressom H, Ahn J, Wolf C, Moussa C. 2020. Discoidin Domain Receptor 1 is a therapeutic target for neurodegenerative diseases. *Human Molecular Genetics* **29**:2882–2898. DOI: https://doi.org/10.1093/hmg/ddaa177, PMID: 32776088

French AJ, Natesampillai S, Krogman A, Correia C, Peterson KL, Alto A, Chandrasekar AP, Misra A, Li Y, Kaufmann SH, Badley AD, Cummins NW. 2020. Reactivating latent HIV with PKC agonists induces resistance to apoptosis and is associated with phosphorylation and activation of BCL2. *PLOS Pathogens* **16**:e1008906. DOI: https://doi.org/10.1371/journal.ppat.1008906, PMID: 33075109

Fuentealba M, Dönertaş HM, Williams R, Labbadia J, Thornton JM, Partridge L. 2019. Using the drug-protein interactome to identify anti-ageing compounds for humans. *PLOS Computational Biology* **15**:e1006639. DOI: https://doi.org/10.1371/journal.pcbi.1006639, PMID: 30625143

Fürstenwerth H. 2012. Rethinking Heart Failure. *Cardiology Research* **3**:243–257. DOI: https://doi.org/10.4021/cr228w, PMID: 28352413

Ganter B, Snyder RD, Halbert DN, Lee MD. 2006. Toxicogenomics in drug discovery and development: mechanistic analysis of compound/class-dependent effects using the DrugMatrix database. *Pharmacogenomics* **7**:1025–1044. DOI: https://doi.org/10.2217/14622416.7.7.1025, PMID: 17054413

Gaudelet T, Day B, Jamasb AR, Soman J, Regep C, Liu G, Hayter JBR, Vickers R, Roberts C, Tang J, Roblin D, Blundell TL, Bronstein MM, Taylor-King JP. 2021. Utilizing graph machine learning within drug discovery and development. *Briefings in Bioinformatics* **22**:1–22. DOI: https://doi.org/10.1093/bib/bbab159, PMID: 34013350

Giorgio C, Incerti M, Pala D, Russo S, Chiodelli P, Rusnati M, Cantoni AM, Di Lecce R, Barocelli E, Bertoni S, Ravassard P, Manenti F, Piemonti L, Ferlenghi F, Lodola A, Tognolini M. 2019. Inhibition of Eph/ephrin interaction with the small molecule UniPR500 improves glucose tolerance in healthy and insulin-resistant mice. *Pharmacological Research* **141**:319–330. DOI: https://doi.org/10.1016/j.phrs.2019.01.011, PMID: 30625359

Gudmundsdottir V, Zaghlool SB, Emilsson V, Aspelund T, Ilkov M, Gudmundsson EF, Jonsson SM, Zilhão NR, Lamb JR, Suhre K, Jennings LL, Gudnason V. 2020. Circulating Protein Signatures and Causal Candidates for Type 2 Diabetes. *Diabetes* **69**:1843–1853. DOI: https://doi.org/10.2337/db19-1070, PMID: 32385057

Guo M, Li Y, Wang Y, Li Z, Li X, Zhao P, Li C, Lv J, Liu X, Du X, Chen Z. 2020. eEF1A2 exacerbated insulin resistance in male skeletal muscle via PKCβ and ER stress. *The Journal of Endocrinology* **244**:25–40. DOI: https://doi.org/10.1530/JOE-19-0051, PMID: 31539873

Gutierrez DA, Vargas LM, Chandia-Cristi A, de la Fuente C, Leal N, Alvarez AR. 2019. c-Abl Deficiency Provides Synaptic Resiliency Against Aβ-Oligomers. *Frontiers in Cellular Neuroscience* **13**:526. DOI: https://doi.org/10.3389/fncel.2019.00526, PMID: 31849613

Herrera Moro Chao D, Wang Y, Foppen E, Ottenhoff R, van Roomen C, Parlevliet ET, van Eijk M, Verhoek M, Boot R, Marques AR, Scheij S, Mirzaian M, Kooijman S, Jansen K, Wang D, Mergen C, Seeley RJ, Tschöp MH, Overkleeft H, Rensen PCN, et al. 2019. The Iminosugar AMP-DNM Improves Satiety and Activates Brown Adipose Tissue Through GLP1. *Diabetes* **68**:2223–2234. DOI: https://doi.org/10.2337/db19-0049, PMID: 31578192

Hevener AL, Zhou Z, Moore TM, Drew BG, Ribas V. 2018. The impact of ERα action on muscle metabolism and insulin sensitivity - Strong enough for a man, made for a woman. *Molecular Metabolism* **15**:20–34. DOI: https://doi.org/10.1016/j.molmet.2018.06.013, PMID: 30005878

Himmelstein DS, Lizee A, Hessler C, Brueggeman L, Chen SL, Hadley D, Green A, Khankhanian P, Baranzini SE. 2017. Systematic integration of biomedical knowledge prioritizes drugs for repurposing. *eLife* **6**:e26726. DOI: https://doi.org/10.7554/eLife.26726, PMID: 28936969

Hoang VT, Nyswaner K, Torres-Ayuso P, Brognard J. 2020. The protein kinase MAP3K19 phosphorylates MAP2Ks and thereby activates ERK and JNK kinases and increases viability of KRAS-mutant lung cancer cells. *The Journal of Biological Chemistry* **295**:8470–8479. DOI: https://doi.org/10.1074/jbc.RA119.012365, PMID: 32358059

Hopkins AL. 2008. Network pharmacology: the next paradigm in drug discovery. *Nature Chemical Biology* **4**:682–690. DOI: https://doi.org/10.1038/nchembio.118, PMID: 18936753

Howell JJ, Hellberg K, Turner M, Talbott G, Kolar MJ, Ross DS, Hoxhaj G, Saghatelian A, Shaw RJ, Manning BD. 2017. Metformin Inhibits Hepatic mTORC1 Signaling via Dose-Dependent Mechanisms Involving AMPK and the TSC Complex. *Cell Metabolism* **25**:463–471. DOI: https://doi.org/10.1016/j.cmet.2016.12.009, PMID: 28089566

Huang K, Fu T, Glass LM, Zitnik M, Xiao C, Sun J. 2021. DeepPurpose: a deep learning library for drug-target interaction prediction. *Bioinformatics* **36**:5545–5547. DOI: https://doi.org/10.1093/bioinformatics/btaa1005, PMID: 33275143

Huh S, Baek SJ, Lee KH, Whitcomb DJ, Jo J, Choi SM, Kim DH, Park MS, Lee KH, Kim BC. 2016. The reemergence of long-term potentiation in aged Alzheimer's disease mouse model. *Scientific Reports* **6**:1–10. DOI: https://doi.org/10.1038/srep29152, PMID: 27377368

Imamura T, Haruta T, Takata Y, Usui I, Iwata M, Ishihara H, Ishiki M, Ishibashi O, Ueno E, Sasaoka T, Kobayashi M. 1998. Involvement of heat shock protein 90 in the degradation of mutant insulin receptors by the proteasome. *The Journal of Biological Chemistry* **273**:11183–11188. DOI: https://doi.org/10.1074/jbc.273.18.11183, PMID: 9556607

Iorio F, Garcia-Alonso L, Brammeld JS, Martincorena I, Wille DR, McDermott U, Saez-Rodriguez J. 2018. Pathway-based dissection of the genomic heterogeneity of cancer hallmarks' acquisition with SLAPenrich. *Scientific Reports* **8**:1–16. DOI: https://doi.org/10.1038/s41598-018-25076-6, PMID: 29713020

Iwai M, Kanno H, Inaba S, Senba I, Sone H, Nakaoka H, Horiuchi M. 2011. Nifedipine, a calcium-channel blocker, attenuated glucose intolerance and white adipose tissue dysfunction in type 2 diabetic KK-A(y) mice. *American Journal of Hypertension* **24**:169–174. DOI: https://doi.org/10.1038/ajh.2010.198, PMID: 20847723

Jahng JWS, Alsaadi RM, Palanivel R, Song E, Hipolito VEB, Sung HK, Botelho RJ, Russell RC, Sweeney G. 2019. Iron overload inhibits late stage autophagic flux leading to insulin resistance. *EMBO Reports* **20**:e47911. DOI: https://doi.org/10.15252/embr.201947911, PMID: 31441223

James T, Sardar A, Anighoro A. 2020. Enhancing Chemogenomics with Predictive Pharmacology. *Journal of Medicinal Chemistry* **63**:12243–12255. DOI: https://doi.org/10.1021/acs.jmedchem.0c00445, PMID: 32573226

Jenkinson CP, Göring HHH, Arya R, Blangero J, Duggirala R, DeFronzo RA. 2016. Transcriptomics in type 2 diabetes: Bridging the gap between genotype and phenotype. *Genomics Data* **8**:25–36. DOI: https://doi.org/10.1016/j.gdata.2015.12.001, PMID: 27114903

Jing E, Sundararajan P, Majumdar ID, Hazarika S, Fowler S, Szeto A, Gesta S, Mendez AJ, Vishnudas VK, Sarangarajan R, Narain NR. 2018. Hsp90β knockdown in DIO mice reverses insulin resistance and improves glucose tolerance. *Nutrition & Metabolism* **15**:11. DOI: https://doi.org/10.1186/s12986-018-0242-6, PMID: 29434648

Karatzas E, Bourdakou MM, Kolios G, Spyrou GM. 2017. Drug repurposing in idiopathic pulmonary fibrosis filtered by a bioinformatics-derived composite score. *Scientific Reports* **7**:12569. DOI: https://doi.org/10.1038/s41598-017-12849-8, PMID: 28974751

Keenan AB, Jenkins SL, Jagodnik KM, Koplev S, He E, Torre D, Wang Z, Dohlman AB, Silverstein MC, Lachmann A, Kuleshov MV, Ma'ayan A, Stathias V, Terryn R, Cooper D, Forlin M, Koleti A, Vidovic D, Chung C, Schürer SC, et al. 2018. The Library of Integrated Network-Based Cellular Signatures NIH Program: System-Level Cataloging of Human Cells Response to Perturbations. *Cell Systems* **6**:13–24. DOI: https://doi.org/10.1016/j.cels.2017.11.001, PMID: 29199020

Kellar D, Craft S. 2020. Brain insulin resistance in Alzheimer's disease and related disorders: mechanisms and therapeutic approaches. *The Lancet. Neurology* **19**:758–766. DOI: https://doi.org/10.1016/S1474-4422(20)30231-3, PMID: 32730766

Klaeger S, Heinzlmeir S, Wilhelm M, Polzer H, Vick B, Koenig PA, Reinecke M, Ruprecht B, Petzoldt S, Meng C, Zecha J, Reiter K, Qiao H, Helm D, Koch H, Schoof M, Canevari G, Casale E, Depaolini SR, Feuchtinger A, et al. 2017. The target landscape of clinical kinase drugs. *Science* **358**:eaan4368. DOI: https://doi.org/10.1126/science.aan4368, PMID: 29191878

Koyama Y, Kodama K, Suzuki M, Harano Y. 2002. Improvement of insulin sensitivity by a long-acting nifedipine preparation (nifedipine-CR) in patients with essential hypertension. *American Journal of Hypertension* **15**:927–931. DOI: https://doi.org/10.1016/s0895-7061(02)03019-4, PMID: 12441210

Kyohara M, Shirakawa J, Okuyama T, Togashi Y, Inoue R, Li J, Miyashita D, Terauchi Y. 2020. Soluble EGFR, a hepatokine, and adipsin, an adipokine, are biomarkers correlated with distinct aspects of insulin resistance in type 2 diabetes subjects. *Diabetology & Metabolic Syndrome* **12**:83. DOI: https://doi.org/10.1186/s13098-020-00591-7, PMID: 33005239

Lee S, Han D, Kang HG, Jeong SJ, Jo JE, Shin J, Kim DK, Park HW. 2019. Intravenous sustained-release nifedipine ameliorates nonalcoholic fatty liver disease by restoring autophagic clearance. *Biomaterials* **197**:1–11. DOI: https://doi.org/10.1016/j.biomaterials.2019.01.008, PMID: 30623792

Lee TH, Chen JL, Liu PS, Tsai MM, Wang SJ, Hsieh HL. 2020. Rottlerin, a natural polyphenol compound, inhibits upregulation of matrix metalloproteinase-9 and brain astrocytic migration by reducing PKC-δ-dependent ROS signal. *Journal of Neuroinflammation* **17**:177. DOI: https://doi.org/10.1186/s12974-020-01859-5, PMID: 32505192

Li M, Vienberg SG, Bezy O, O'Neill BT, Kahn CR. 2015. Role of PKCδ in Insulin Sensitivity and Skeletal Muscle Metabolism. *Diabetes* **64**:4023–4032. DOI: https://doi.org/10.2337/db14-1891, PMID: 26307588

Li S, Wang C, Li K, Li L, Tian M, Xie J, Yang M, Jia Y, He J, Gao L, Boden G, Liu H, Yang G. 2016. NAMPT knockdown attenuates atherosclerosis and promotes reverse cholesterol transport in ApoE KO mice with high-fat-induced insulin resistance. *Scientific Reports* **6**:26746. DOI: https://doi.org/10.1038/srep26746, PMID: 27229177

Li T, Kim A, Rosenbluh J, Horn H, Greenfeld L, An D, Zimmer A, Liberzon A, Bistline J, Natoli T, Li Y, Tsherniak A, Narayan R, Subramanian A, Liefeld T, Wong B, Thompson D, Calvo S, Carr S, Boehm J, et al. 2018a. GeNets: a unified web platform for network-based genomic analyses. *Nature Methods* **15**:543–546. DOI: https://doi.org/10.1038/s41592-018-0039-6, PMID: 29915188

Li Z, Li Y, Overstreet JM, Chung S, Niu A, Fan X, Wang S, Wang Y, Zhang MZ, Harris RC. 2018b. Inhibition of Epidermal Growth Factor Receptor Activation Is Associated With Improved Diabetic Nephropathy and Insulin Resistance in Type 2 Diabetes. *Diabetes* **67**:1847–1857. DOI: https://doi.org/10.2337/db17-1513, PMID: 29959129

Liu T, Lin Y, Wen X, Jorissen RN, Gilson MK. 2007. BindingDB: a web-accessible database of experimentally determined protein-ligand binding affinities. *Nucleic Acids Research* **35**:D198–D201. DOI: https://doi.org/10.1093/nar/gkl999, PMID: 17145705

Liu W, Tian X, Wu T, Liu L, Guo Y, Wang C. 2019. PDE5A Suppresses Proteasome Activity Leading to Insulin Resistance in C2C12 Myotubes. *International Journal of Endocrinology* **2019**:3054820. DOI: https://doi.org/10.1155/2019/3054820, PMID: 30774657

Lockman JW, Murphy BR, Zigar DF, Judd WR, Slattum PM, Gao ZH, Ostanin K, Green J, McKinnon R, Terry-Lorenzo RT, Fleischer TC, Boniface JJ, Shenderovich M, Willardsen JA. 2010. Analogues of 4-[(7-Bromo-2-methyl-4-oxo-3H-quinazolin-6-yl)methylprop-2-ynylamino]-N-(3-pyridylmethyl)benzamide (CB-30865) as potent inhibitors of nicotinamide phosphoribosyltransferase (Nampt). *Journal of Medicinal Chemistry* **53**:8734–8746. DOI: https://doi.org/10.1021/jm101145b, PMID: 21080724

Lotta LA, Gulati P, Day FR, Payne F, Ongen H, van de Bunt M, Gaulton KJ, Eicher JD, Sharp SJ, Luan J, De Lucia Rolfe E, Stewart ID, Wheeler E, Willems SM, Adams C, Yaghootkar H, EPIC-InterAct Consortium, Cambridge FPLD1 Consortium, Forouhi NG, Khaw KT, et al. 2017. Integrative genomic analysis implicates limited peripheral adipose storage capacity in the pathogenesis of human insulin resistance. *Nature Genetics* **49**:17–26. DOI: https://doi.org/10.1038/ng.3714, PMID: 27841877

Luk CT, Shi SY, Cai EP, Sivasubramaniyam T, Krishnamurthy M, Brunt JJ, Schroer SA, Winer DA, Woo M. 2017. FAK signalling controls insulin sensitivity through regulation of adipocyte survival. *Nature Communications* **8**:14360. DOI: https://doi.org/10.1038/ncomms14360, PMID: 28165007

MacLaren R, Cui W, Simard S, Cianflone K. 2008. Influence of obesity and insulin sensitivity on insulin signaling genes in human omental and subcutaneous adipose tissue. *Journal of Lipid Research* **49**:308–323. DOI: https://doi.org/10.1194/jlr.M700199-JLR200, PMID: 17986714

Martins VF, Begur M, Lakkaraju S, Svensson K, Park J, Hetrick B, McCurdy CE, Schenk S. 2019. Acute inhibition of protein deacetylases does not impact skeletal muscle insulin action. *American Journal of Physiology. Cell Physiology* **317**:C964–C968. DOI: https://doi.org/10.1152/ajpcell.00159.2019, PMID: 31461343

Menden MP, Wang D, Mason MJ, Szalai B, Bulusu KC, Guan Y, Yu T, Kang J, Jeon M, Wolfinger R, Nguyen T, Zaslavskiy M, AstraZeneca-Sanger Drug Combination DREAM Consortium, Jang IS, Ghazoui Z, Ahsen ME, Vogel R, Neto EC, Norman T, Tang EKY, et al. 2019. Community assessment to advance computational prediction of cancer drug combinations in a pharmacogenomic screen. *Nature Communications* **10**:1–17. DOI: https://doi.org/10.1038/s41467-019-09799-2, PMID: 31209238

Mendez D, Gaulton A, Bento AP, Chambers J, De Veij M, Félix E, Magariños MP, Mosquera JF, Mutowo P, Nowotka M, Gordillo-Marañón M, Hunter F, Junco L, Mugumbate G, Rodriguez-Lopez M, Atkinson F, Bosc N, Radoux CJ, Segura-Cabrera A, Hersey A, et al. 2019. ChEMBL: towards direct deposition of bioassay data. *Nucleic Acids Research* **47**:D930–D940. DOI: https://doi.org/10.1093/nar/gky1075, PMID: 30398643

Moret N, Clark NA, Hafner M, Wang Y, Lounkine E, Medvedovic M, Wang J, Gray N, Jenkins J, Sorger PK. 2019. Cheminformatics Tools for Analyzing and Designing Optimized Small-Molecule Collections and Libraries. *Cell Chemical Biology* **26**:765–777. DOI: https://doi.org/10.1016/j.chembiol.2019.02.018, PMID: 30956147

Morita M, Gravel SP, Chénard V, Sikström K, Zheng L, Alain T, Gandin V, Avizonis D, Arguello M, Zakaria C, McLaughlan S, Nouet Y, Pause A, Pollak M, Gottlieb E, Larsson O, St-Pierre J, Topisirovic I, Sonenberg N. 2013. mTORC1 controls mitochondrial activity and biogenesis through 4E-BP-dependent translational regulation. *Cell Metabolism* **18**:698–711. DOI: https://doi.org/10.1016/j.cmet.2013.10.001, PMID: 24206664

Musso G, Cassader M, De Michieli F, Paschetta E, Pinach S, Saba F, Bongiovanni D, Framarin L, Berrutti M, Leone N, Corvisieri S, Parente R, Molinaro F, Sircana A, Bo S, Gambino R. 2017. MERTK rs4374383 variant predicts incident nonalcoholic fatty liver disease and diabetes: role of mononuclear cell activation and adipokine response to dietary fat. *Human Molecular Genetics* **26**:1747–1758. DOI: https://doi.org/10.1093/hmg/ddw400, PMID: 28334911

Nakhuda A, Josse AR, Gburcik V, Crossland H, Raymond F, Metairon S, Good L, Atherton PJ, Phillips SM, Timmons JA. 2016. Biomarkers of browning of white adipose tissue and their regulation. *The American Journal of Clinical Nutrition* 1:557–565. DOI: https://doi.org/10.3945/ajcn.116.132563

Naruse K, Rask-Madsen C, Takahara N, Ha S, Suzuma K, Way KJ, Jacobs JRC, Clermont AC, Ueki K, Ohshiro Y, Zhang J, Goldfine AB, King GL. 2006. Activation of vascular protein kinase C-beta inhibits Akt-dependent endothelial nitric oxide synthase function in obesity-associated insulin resistance. *Diabetes* 55:691–698. DOI: https://doi.org/10.2337/diabetes.55.03.06.db05-0771, PMID: 16505232

Nie C, He T, Zhang W, Zhang G, Ma X. 2018a. Branched Chain Amino Acids: Beyond Nutrition Metabolism. *International Journal of Molecular Sciences* 19:E954. DOI: https://doi.org/10.3390/ijms19040954, PMID: 29570613

Nie SD, Li X, Tang CE, Min FY, Shi XJ, Wu LY, Zhou SL, Chen Z, Wu J, Song T, Dai ZJ, Zheng J, Liu JJ, Wang S. 2018b. High glucose forces a positive feedback loop connecting ErbB4 expression and mTOR/S6K pathway to aggravate the formation of tau hyperphosphorylation in differentiated SH-SY5Y cells. *Neurobiology of Aging* 67:171–180. DOI: https://doi.org/10.1016/j.neurobiolaging.2018.03.023, PMID: 29674181

Norambuena A, Wallrabe H, McMahon L, Silva A, Swanson E, Khan SS, Baerthlein D, Kodis E, Oddo S, Mandell JW, Bloom GS. 2017. mTOR and neuronal cell cycle reentry: How impaired brain insulin signaling promotes Alzheimer's disease. *Alzheimer's & Dementia* 13:152–167. DOI: https://doi.org/10.1016/j.jalz.2016.08.015, PMID: 27693185

Osrodek M, Rozanski M, Czyz M. 2020. Insulin Reduces the Efficacy of Vemurafenib and Trametinib in Melanoma Cells. *Cancer Management and Research* 12:7231–7250. DOI: https://doi.org/10.2147/CMAR.S263767, PMID: 32982400

Ozaki KI, Awazu M, Tamiya M, Iwasaki Y, Harada A, Kugisaki S, Tanimura S, Kohno M. 2016. Targeting the ERK signaling pathway as a potential treatment for insulin resistance and type 2 diabetes. *American Journal of Physiology. Endocrinology and Metabolism* 310:E643–E651. DOI: https://doi.org/10.1152/ajpendo.00445.2015, PMID: 26860984

Ozcan Lale, Cristina de Souza J, Harari AA, Backs J, Olson EN, Tabas I. 2013. Activation of calcium/calmodulin-dependent protein kinase II in obesity mediates suppression of hepatic insulin signaling. *Cell Metabolism* 18:803–815. DOI: https://doi.org/10.1016/j.cmet.2013.10.011, PMID: 24268736

Ozcan L, Xu X, Deng SX, Ghorpade DS, Thomas T, Cremers S, Hubbard B, Serrano-Wu MH, Gaestel M, Landry DW, Tabas I. 2015. Treatment of Obese Insulin-Resistant Mice With an Allosteric MAPKAPK2/3 Inhibitor Lowers Blood Glucose and Improves Insulin Sensitivity. *Diabetes* 64:3396–3405. DOI: https://doi.org/10.2337/db14-1945, PMID: 26068544

Palacio-Rodríguez K, Lans I, Cavasotto CN, Cossio P. 2019. Exponential consensus ranking improves the outcome in docking and receptor ensemble docking. *Scientific Reports* 9:5142. DOI: https://doi.org/10.1038/s41598-019-41594-3, PMID: 30914702

Parisi D, Adasme MF, Sveshnikova A, Bolz SN, Moreau Y, Schroeder M. 2020. Drug repositioning or target repositioning: A structural perspective of drug-target-indication relationship for available repurposed drugs. *Computational and Structural Biotechnology Journal* 18:1043–1055. DOI: https://doi.org/10.1016/j.csbj.2020.04.004, PMID: 32419905

Park S, Hong SM, Lee JE. 2007. Chlorpromazine exacerbates hepatic insulin sensitivity via attenuating insulin and leptin signaling pathway, while exercise partially reverses the adverse effects. *Life Sciences* 80:2428–2435. DOI: https://doi.org/10.1016/j.lfs.2007.04.001

Perez-Castillo Y, Helguera AM, Cordeiro M, Tejera E, Paz-Y-Mino C, Sanchez-Rodriguez A, Borges F, Cruz-Monteagudo M. 2017. Fusing Docking Scoring Functions Improves the Virtual Screening Performance for Discovering Parkinson's Disease Dual Target Ligands. *Current Neuropharmacology* 15:1107–1116. DOI: https://doi.org/10.2174/1570159X15666170109143757, PMID: 28067172

Phillips BE, Kelly BM, Lilja M, Ponce-González JG, Brogan RJ, Morris DL, Gustafsson T, Kraus WE, Atherton PJ, Vollaard NBJ, Rooyackers O, Timmons JA. 2017. A Practical and Time-Efficient High-Intensity Interval Training Program Modifies Cardio-Metabolic Risk Factors in Adults with Risk Factors for Type II Diabetes. *Frontiers in Endocrinology* 8:1–11. DOI: https://doi.org/10.3389/fendo.2017.00229, PMID: 28943861

Reading CL, Stickney DR, Flores-Riveros J, Destiche DA, Ahlem CN, Cefalu WT, Frincke JM. 2013. A synthetic anti-inflammatory sterol improves insulin sensitivity in insulin-resistant obese impaired glucose tolerance subjects. *Obesity* 21:E343–E349. DOI: https://doi.org/10.1002/oby.20207, PMID: 23670958

Redhead MA, Owen CD, Brewitz L, Collette AH, Lukacik P, Strain-Damerell C, Robinson SW, Collins PM, Schäfer P, Swindells M, Radoux CJ, Hopkins IN, Fearon D, Douangamath A, von Delft F, Malla TR, Vangeel L, Vercruysse T, Thibaut J, Leyssen P, et al. 2021. Bispecific repurposed medicines targeting the viral and immunological arms of COVID-19. *Scientific Reports* 11:1–14. DOI: https://doi.org/10.1038/s41598-021-92416-4, PMID: 34168183

Regan-Fendt KE, Xu J, DiVincenzo M, Duggan MC, Shakya R, Na R, Carson WE, Payne PRO, Li F. 2019. Synergy from gene expression and network mining (SynGeNet) method predicts synergistic drug combinations for diverse melanoma genomic subtypes. *NPJ Systems Biology and Applications* 5:6. DOI: https://doi.org/10.1038/s41540-019-0085-4, PMID: 30820351

Sajan MP, Hansen BC, Higgs MG, Kahn CR, Braun U, Leitges M, Park CR, Diamond DM, Farese RV. 2018. Atypical PKC, PKC λ / ι, activates β-secretase and increases Aβ1-40/42 and phospho-tau in mouse brain and isolated neuronal cells, and may link hyperinsulinemia and other aPKC activators to development of pathological and memory abnormalities in Alzheimer's disease. *Neurobiology of Aging* 61:225–237. DOI: https://doi.org/10.1016/j.neurobiolaging.2017.09.001, PMID: 29032894

Sartor GC, Malvezzi AM, Kumar A, Andrade NS, Wiedner HJ, Vilca SJ, Janczura KJ, Bagheri A, Al-Ali H, Powell SK, Brown PT, Volmar CH, Foster TC, Zeier Z, Wahlestedt C. 2019. Enhancement of BDNF Expression and Memory by HDAC Inhibition Requires BET Bromodomain Reader Proteins. *The Journal of Neuroscience* **39**:612–626. DOI: https://doi.org/10.1523/JNEUROSCI.1604-18.2018, PMID: 30504275

Sears DD, Hsiao G, Hsiao A, Yu JG, Courtney CH, Ofrecio JM, Chapman J, Subramaniam S. 2009. Mechanisms of human insulin resistance and thiazolidinedione-mediated insulin sensitization. *PNAS* **106**:18745–18750. DOI: https://doi.org/10.1073/pnas.0903032106, PMID: 19841271

Sharma MK, Jalewa J, Hölscher C. 2014. Neuroprotective and anti-apoptotic effects of liraglutide on SH-SY5Y cells exposed to methylglyoxal stress. *Journal of Neurochemistry* **128**:459–471. DOI: https://doi.org/10.1111/jnc.12469, PMID: 24112036

Sharma A, Maurya CK, Arha D, Rai AK, Singh S, Varshney S, Schertzer JD, Tamrakar AK. 2019. Nod1-mediated lipolysis promotes diacylglycerol accumulation and successive inflammation via PKCδ-IRAK axis in adipocytes. *Biochimica et Biophysica Acta. Molecular Basis of Disease* **1865**:136–146. DOI: https://doi.org/10.1016/j.bbadis.2018.10.036, PMID: 30391544

Shelton LB, Baker JD, Zheng D, Sullivan LE, Solanki PK, Webster JM, Sun Z, Sabbagh JJ, Nordhues BA, Koren J, Ghosh S, Blagg BSJ, Blair LJ, Dickey CA. 2017. Hsp90 activator Aha1 drives production of pathological tau aggregates. *PNAS* **114**:9707–9712. DOI: https://doi.org/10.1073/pnas.1707039114, PMID: 28827321

Sheu WH, Swislocki ALM, Hoffman B, Chen YDI, Reaven GM. 1991. Comparison of the effects of atenolol and nifedipine on glucose, insulin, and lipid metabolism in patients with hypertension. *American Journal of Hypertension* **4**:199–205. DOI: https://doi.org/10.1093/ajh/4.3.199, PMID: 2043298

Skurski J, Penniman CM, Geesala R, Dixit G, Pulipati P, Bhardwaj G, Meyerholz DK, Issuree PD, O'Neill BT, Maretzky T. 2020. Loss of iRhom2 accelerates fat gain and insulin resistance in diet-induced obesity despite reduced adipose tissue inflammation. *Metabolism* **106**:154194. DOI: https://doi.org/10.1016/j.metabol.2020.154194, PMID: 32135161

Slentz CA, Bateman LA, Willis LH, Shields AT, Tanner CJ, Piner LW, Hawk VH, Muehlbauer MJ, Samsa GP, Nelson RC, Huffman KM, Bales CW, Houmard JA, Kraus WE. 2011. Effects of aerobic vs. resistance training on visceral and liver fat stores, liver enzymes, and insulin resistance by HOMA in overweight adults from STRRIDE AT/RT. *American Journal of Physiology. Endocrinology and Metabolism* **301**:E1033–E1039. DOI: https://doi.org/10.1152/ajpendo.00291.2011, PMID: 21846904

Slentz CA, Bateman LA, Willis LH, Granville EO, Piner LW, Samsa GP, Setji TL, Muehlbauer MJ, Huffman KM, Bales CW, Kraus WE. 2016. Effects of exercise training alone vs a combined exercise and nutritional lifestyle intervention on glucose homeostasis in prediabetic individuals: a randomised controlled trial. *Diabetologia* **59**:2088–2098. DOI: https://doi.org/10.1007/s00125-016-4051-z, PMID: 27421729

Song WM, Zhang B. 2015. Multiscale Embedded Gene Co-expression Network Analysis. *PLOS Computational Biology* **11**:e1004574. DOI: https://doi.org/10.1371/journal.pcbi.1004574, PMID: 26618778

Sood S, Szkop KJ, Nakhuda A, Gallagher IJ, Murie C, Brogan RJ, Kaprio J, Kainulainen H, Atherton PJ, Kujala UM, Gustafsson T, Larsson O, Timmons JA. 2016. iGEMS: an integrated model for identification of alternative exon usage events. *Nucleic Acids Research* **44**:1–14. DOI: https://doi.org/10.1093/nar/gkw263, PMID: 27095197

Stathias V, Turner J, Koleti A, Vidovic D, Cooper D, Fazel-Najafabadi M, Pilarczyk M, Terryn R, Chung C, Umeano A, Clarke DJB, Lachmann A, Evangelista JE, Ma'ayan A, Medvedovic M, Schürer SC. 2020. LINCS Data Portal 2.0: next generation access point for perturbation-response signatures. *Nucleic Acids Research* **48**:D431–D439. DOI: https://doi.org/10.1093/nar/gkz1023, PMID: 31701147

Stoelzel CR, Zhang Y, Cincotta AH. 2020. Circadian-timed dopamine agonist treatment reverses high-fat diet-induced diabetogenic shift in ventromedial hypothalamic glucose sensing. *Endocrinology, Diabetes & Metabolism* **3**:e00139. DOI: https://doi.org/10.1002/edm2.139, PMID: 32704560

Stokes T, Timmons JA, Crossland H, Tripp TR, Murphy K, McGlory C, Mitchell CJ, Oikawa SY, Morton RW, Phillips BE, Baker SK, Atherton PJ, Wahlestedt C, Phillips SM. 2020. Molecular Transducers of Human Skeletal Muscle Remodeling under Different Loading States. *Cell Reports* **32**:107980. DOI: https://doi.org/10.1016/j.celrep.2020.107980, PMID: 32755574

Sturm N, Mayr A, Le Van T, Chupakhin V, Ceulemans H, Wegner J, Golib-Dzib JF, Jeliazkova N, Vandriessche Y, Böhm S, Cima V, Martinovic J, Greene N, Vander Aa T, Ashby TJ, Hochreiter S, Engkvist O, Klambauer G, Chen H. 2020. Industry-scale application and evaluation of deep learning for drug target prediction. *Journal of Cheminformatics* **12**:26. DOI: https://doi.org/10.1186/s13321-020-00428-5, PMID: 33430964

Subramanian A, Narayan R, Corsello SM, Peck DD, Natoli TE, Lu X, Gould J, Davis JF, Tubelli AA, Asiedu JK, Lahr DL, Hirschman JE, Liu Z, Donahue M, Julian B, Khan M, Wadden D, Smith IC, Lam D, Liberzon A, et al. 2017. A Next Generation Connectivity Map: L1000 Platform and the First 1,000,000 Profiles. *Cell* **171**:1437–1452. DOI: https://doi.org/10.1016/j.cell.2017.10.049, PMID: 29195078

Sun YBY, Qu X, Howard V, Dai L, Jiang X, Ren Y, Fu P, Puelles VG, Nikolic-Paterson DJ, Caruana G, Bertram JF, Sleeman MW, Li J. 2015. Smad3 deficiency protects mice from obesity-induced podocyte injury that precedes insulin resistance. *Kidney International* **88**:286–298. DOI: https://doi.org/10.1038/ki.2015.121, PMID: 25945408

Sun X, Li J, Sun Y, Zhang Y, Dong L, Shen C, Yang L, Yang M, Li Y, Shen G, Tu Y, Tao J. 2016. miR-7 reverses the resistance to BRAFi in melanoma by targeting EGFR/IGF-1R/CRAF and inhibiting the MAPK and PI3K/AKT signaling pathways. *Oncotarget* **7**:53558–53570. DOI: https://doi.org/10.18632/oncotarget.10669, PMID: 27448964

Tan CK, Leuenberger N, Tan MJ, Yan YW, Chen Y, Kambadur R, Wahli W, Tan NS. 2011. Smad3 deficiency in mice protects against insulin resistance and obesity induced by a high-fat diet. *Diabetes* **60**:464–476. DOI: https://doi.org/10.2337/db10-0801, PMID: 21270259

Tan MS, Yang YX, Xu W, Wang HF, Tan L, Zuo CT, Dong Q, Tan L, Suckling J, Yu JT, Alzheimer's Disease Neuroimaging Initiative. 2021. Associations of Alzheimer's disease risk variants with gene expression, amyloidosis, tauopathy, and neurodegeneration. *Alzheimer's Research & Therapy* **13**:15. DOI: https://doi.org/10.1186/s13195-020-00755-7, PMID: 33419465

Tang J, Szwajda A, Shakyawar S, Xu T, Hintsanen P, Wennerberg K, Aittokallio T. 2014. Making sense of large-scale kinase inhibitor bioactivity data sets: a comparative and integrative analysis. *Journal of Chemical Information and Modeling* **54**:735–743. DOI: https://doi.org/10.1021/ci400709d, PMID: 24521231

Tarragó MG, Chini CCS, Kanamori KS, Warner GM, Caride A, de Oliveira GC, Rud M, Samani A, Hein KZ, Huang R, Jurk D, Cho DS, Boslett JJ, Miller JD, Zweier JL, Passos JF, Doles JD, Becherer DJ, Chini EN. 2018. A Potent and Specific CD38 Inhibitor Ameliorates Age-Related Metabolic Dysfunction by Reversing Tissue NAD+ Decline. *Cell Metabolism* **27**:1081–1095. DOI: https://doi.org/10.1016/j.cmet.2018.03.016, PMID: 29719225

Timmons JA, Larsson O, Jansson E, Fischer H, Gustafsson T, Greenhaff PL, Ridden J, Rachman J, Peyrard-Janvid M, Wahlestedt C, Sundberg CJ. 2005. Human muscle gene expression responses to endurance training provide a novel perspective on Duchenne muscular dystrophy. *FASEB Journal* **19**:750–760. DOI: https://doi.org/10.1096/fj.04-1980com, PMID: 15857889

Timmons JA, Szkop KJ, Gallagher IJ. 2015. Multiple sources of bias confound functional enrichment analysis of global -omics data. *Genome Biology* **16**:15–17. DOI: https://doi.org/10.1186/s13059-015-0761-7, PMID: 26346307

Timmons JA, Atherton PJ, Larsson O, Sood S, Blokhin IO, Brogan RJ, Volmar CH, Josse AR, Slentz C, Wahlestedt C, Phillips SM, Phillips BE, Gallagher IJ, Kraus WE. 2018. A coding and non-coding transcriptomic perspective on the genomics of human metabolic disease. *Nucleic Acids Research* **46**:7772–7792. DOI: https://doi.org/10.1093/nar/gky570, PMID: 29986096

Timmons JA, Volmar CH, Crossland H, Phillips BE, Sood S, Janczura KJ, Törmäkangas T, Kujala UM, Kraus WE, Atherton PJ, Wahlestedt C. 2019. Longevity-related molecular pathways are subject to midlife "switch" in humans. *Aging Cell* **18**:1–10. DOI: https://doi.org/10.1111/acel.12970, PMID: 31168962

Travelli C, Aprile S, Rahimian R, Grolla AA, Rogati F, Bertolotti M, Malagnino F, di Paola R, Impellizzeri D, Fusco R, Mercalli V, Massarotti A, Stortini G, Terrazzino S, Del Grosso E, Fakhfouri G, Troiani MP, Alisi MA, Grosa G, Sorba G, et al. 2017. Identification of Novel Triazole-Based Nicotinamide Phosphoribosyltransferase (NAMPT) Inhibitors Endowed with Antiproliferative and Antiinflammatory Activity. *Journal of Medicinal Chemistry* **60**:1768–1792. DOI: https://doi.org/10.1021/acs.jmedchem.6b01392, PMID: 28165742

Triana-Martínez F, Picallos-Rabina P, Da Silva-Álvarez S, Pietrocola F, Llanos S, Rodilla V, Soprano E, Pedrosa P, Ferreirós A, Barradas M, Hernández-González F, Lalinde M, Prats N, Bernadó C, González P, Gómez M, Ikonomopoulou MP, Fernández-Marcos PJ, García-Caballero T, Del Pino P, et al. 2019. Identification and characterization of Cardiac Glycosides as senolytic compounds. *Nature Communications* **10**:4731. DOI: https://doi.org/10.1038/s41467-019-12888-x, PMID: 31636264

Um SH, Frigerio F, Watanabe M, Picard F, Joaquin M, Sticker M, Fumagalli S, Allegrini PR, Kozma SC, Auwerx J, Thomas G. 2004. Absence of S6K1 protects against age- and diet-induced obesity while enhancing insulin sensitivity. *Nature* **431**:200–205. DOI: https://doi.org/10.1038/nature02866, PMID: 15306821

Vella V, Malaguarnera R, Nicolosi ML, Morrione A, Belfiore A. 2019. Insulin/IGF signaling and discoidin domain receptors: An emerging functional connection. *Biochimica et Biophysica Acta. Molecular Cell Research* **1866**:118522. DOI: https://doi.org/10.1016/j.bbamcr.2019.118522, PMID: 31394114

Volmar CH, Salah-Uddin H, Janczura KJ, Halley P, Lambert G, Wodrich A, Manoah S, Patel NH, Sartor GC, Mehta N, Miles NTH, Desse S, Dorcius D, Cameron MD, Brothers SP, Wahlestedt C. 2017. M344 promotes nonamyloidogenic amyloid precursor protein processing while normalizing Alzheimer's disease genes and improving memory. *PNAS* **114**:E9135–E9144. DOI: https://doi.org/10.1073/pnas.1707544114, PMID: 29073110

Vujkovic M, Keaton JM, Lynch JA, Miller DR, Zhou J, Tcheandjieu C, Huffman JE, Assimes TL, Lorenz K, Zhu X, Hilliard AT, Judy RL, Huang J, Lee KM, Klarin D, Pyarajan S, Danesh J, Melander O, Rasheed A, Mallick NH, et al. 2020. Discovery of 318 new risk loci for type 2 diabetes and related vascular outcomes among 1.4 million participants in a multi-ancestry meta-analysis. *Nature Genetics* **52**:680–691. DOI: https://doi.org/10.1038/s41588-020-0637-y, PMID: 32541925

Wagner A, Cohen N, Kelder T, Amit U, Liebman E, Steinberg DM, Radonjic M, Ruppin E. 2015. Drugs that reverse disease transcriptomic signatures are more effective in a mouse model of dyslipidemia. *Molecular Systems Biology* **11**:791. DOI: https://doi.org/10.15252/msb.20145486, PMID: 26148350

Wallace TM, Levy JC, Matthews DR, Homa T. 2004. Use and abuse of HOMA modeling. *Diabetes Care* **27**:1487–1495. DOI: https://doi.org/10.2337/diacare.27.6.1487, PMID: 15161807

Wamil M, Coleman RL, Adler AI, McMurray JJV, Holman RR. 2021. Increased Risk of Incident Heart Failure and Death Is Associated With Insulin Resistance in People With Newly Diagnosed Type 2 Diabetes: UKPDS 89. *Diabetes Care* **44**:1877–1884. DOI: https://doi.org/10.2337/dc21-0429, PMID: 34162666

Wang L, Chiang HC, Wu W, Liang B, Xie Z, Yao X, Ma W, Du S, Zhong Y. 2012. Epidermal growth factor receptor is a preferred target for treating amyloid-β-induced memory loss. *PNAS* **109**:16743–16748. DOI: https://doi.org/10.1073/pnas.1208011109, PMID: 23019586

Wang Z, Monteiro CD, Jagodnik KM, Fernandez NF, Gundersen GW, Rouillard AD, Jenkins SL, Feldmann AS, Hu KS, McDermott MG, Duan Q, Clark NR, Jones MR, Kou Y, Goff T, Woodland H, Amaral FMR, Szeto GL, Fuchs O, Schüssler-Fiorenza Rose SM, et al. 2016. Extraction and analysis of signatures from the Gene

Expression Omnibus by the crowd. *Nature Communications* 7:1–11. DOI: https://doi.org/10.1038/ncomms12846, PMID: 27667448

Wang K, Liang Y, Su Y, Wang L. 2020. DhHP-6 ameliorates hepatic oxidative stress and insulin resistance in type 2 diabetes mellitus through the PI3K/AKT and AMPK pathway. *The Biochemical Journal* 477:2363–2381. DOI: https://doi.org/10.1042/BCJ20200402, PMID: 32510127

Wauson EM, Guerra ML, Barylko B, Albanesi JP, Cobb MH. 2013. Off-target effects of MEK inhibitors. *Biochemistry* 52:5164–5166. DOI: https://doi.org/10.1021/bi4007644, PMID: 23848362

Welsh EA, Eschrich SA, Berglund AE, Fenstermacher DA. 2013. Iterative rank-order normalization of gene expression microarray data. *BMC Bioinformatics* 14:153. DOI: https://doi.org/10.1186/1471-2105-14-153, PMID: 23647742

Williams G, Gatt A, Clarke E, Corcoran J, Doherty P, Chambers D, Ballard C. 2019. Drug repurposing for Alzheimer's disease based on transcriptional profiling of human iPSC-derived cortical neurons. *Translational Psychiatry* 9:220. DOI: https://doi.org/10.1038/s41398-019-0555-x, PMID: 31492831

Woo RS, Lee JH, Yu HN, Song DY, Baik TK. 2011. Expression of ErbB4 in the neurons of Alzheimer's disease brain and APP/PS1 mice, a model of Alzheimer's disease. *Anatomy & Cell Biology* 44:116–127. DOI: https://doi.org/10.5115/acb.2011.44.2.116, PMID: 21829755

Woo JH, Shimoni Y, Yang WS, Subramaniam P, Iyer A, Nicoletti P, Rodríguez Martínez M, López G, Mattioli M, Realubit R, Karan C, Stockwell BR, Bansal M, Califano A. 2015. Elucidating Compound Mechanism of Action by Network Perturbation Analysis. *Cell* 162:441–451. DOI: https://doi.org/10.1016/j.cell.2015.05.056, PMID: 26186195

Wu R, Sun JG, Wang JQ, Li B, Liu Q, Ning G, Jin W, Yuan Z. 2017. c-Abl inhibition mitigates diet-induced obesity through improving insulin sensitivity of subcutaneous fat in mice. *Diabetologia* 60:900–910. DOI: https://doi.org/10.1007/s00125-016-4202-2, PMID: 28074253

Xu C, Ai D, Suo S, Chen X, Yan Y, Cao Y, Sun N, Chen W, McDermott J, Zhang S, Zeng Y, Han JDJ. 2018. Accurate Drug Repositioning through Non-tissue-Specific Core Signatures from Cancer Transcriptomes. *Cell Reports* 25:523–535. DOI: https://doi.org/10.1016/j.celrep.2018.09.031

Yang J, Roe SM, Cliff MJ, Williams MA, Ladbury JE, Cohen PTW, Barford D. 2005. Molecular basis for TPR domain-mediated regulation of protein phosphatase 5. *The EMBO Journal* 24:1–10. DOI: https://doi.org/10.1038/sj.emboj.7600496, PMID: 15577939

Yang JK, Lu J, Yuan SS, Cao X, Qiu HY, Shi TT, Yang FY, Li Q, Liu CP, Wu Q, Wang YH, Huang HX, Kayoumu A, Feng JP, Xie RR, Zhu XR, Liu C, Yang GR, Zhang MR, Xie CL, et al. 2018. From Hyper- to Hypoinsulinemia and Diabetes: Effect of KCNH6 on Insulin Secretion. *Cell Reports* 25:3800–3810. DOI: https://doi.org/10.1016/j.celrep.2018.12.005, PMID: 30590050

Yin P, Xu H, Wang Q, Wang J, Yin L, Xu M, Xie Z, Liu W, Cao X. 2017. Overexpression of βCaMKII impairs behavioral flexibility and NMDAR-dependent long-term depression in the dentate gyrus. *Neuropharmacology* 116:270–287. DOI: https://doi.org/10.1016/j.neuropharm.2016.12.013, PMID: 27993520

Yu Y, Ross SA, Halseth AE, Hollenbach PW, Hill RJ, Gulve EA, Bond BR. 2005. Role of PYK2 in the development of obesity and insulin resistance. *Biochemical and Biophysical Research Communications* 334:1085–1091. DOI: https://doi.org/10.1016/j.bbrc.2005.06.198, PMID: 16039993

Zeng X, Zhu S, Lu W, Liu Z, Huang J, Zhou Y, Fang J, Huang Y, Guo H, Li L, Trapp BD, Nussinov R, Eng C, Loscalzo J, Cheng F. 2020. Target identification among known drugs by deep learning from heterogeneous networks. *Chemical Science* 11:1775–1797. DOI: https://doi.org/10.1039/c9sc04336e, PMID: 34123272

Zhan J, Chitta RK, Harwood FC, Grosveld GC. 2019. Phosphorylation of TSC2 by PKC-δ reveals a novel signaling pathway that couples protein synthesis to mTORC1 activity. *Molecular and Cellular Biochemistry* 456:123–134. DOI: https://doi.org/10.1007/s11010-019-03498-8, PMID: 30684133

Zhou Y, Zhou B, Pache L, Chang M, Khodabakhshi AH, Tanaseichuk O, Benner C, Chanda SK. 2019. Metascape provides a biologist-oriented resource for the analysis of systems-level datasets. *Nature Communications* 10:1523. DOI: https://doi.org/10.1038/s41467-019-09234-6, PMID: 30944313

Zou MH, Kirkpatrick SS, Davis BJ, Nelson JS, Wiles WG, Schlattner U, Neumann D, Brownlee M, Freeman MB, Goldman MH. 2004. Activation of the AMP-activated protein kinase by the anti-diabetic drug metformin in vivo. Role of mitochondrial reactive nitrogen species. *The Journal of Biological Chemistry* 279:43940–43951. DOI: https://doi.org/10.1074/jbc.M404421200, PMID: 15265871

Appendix 1

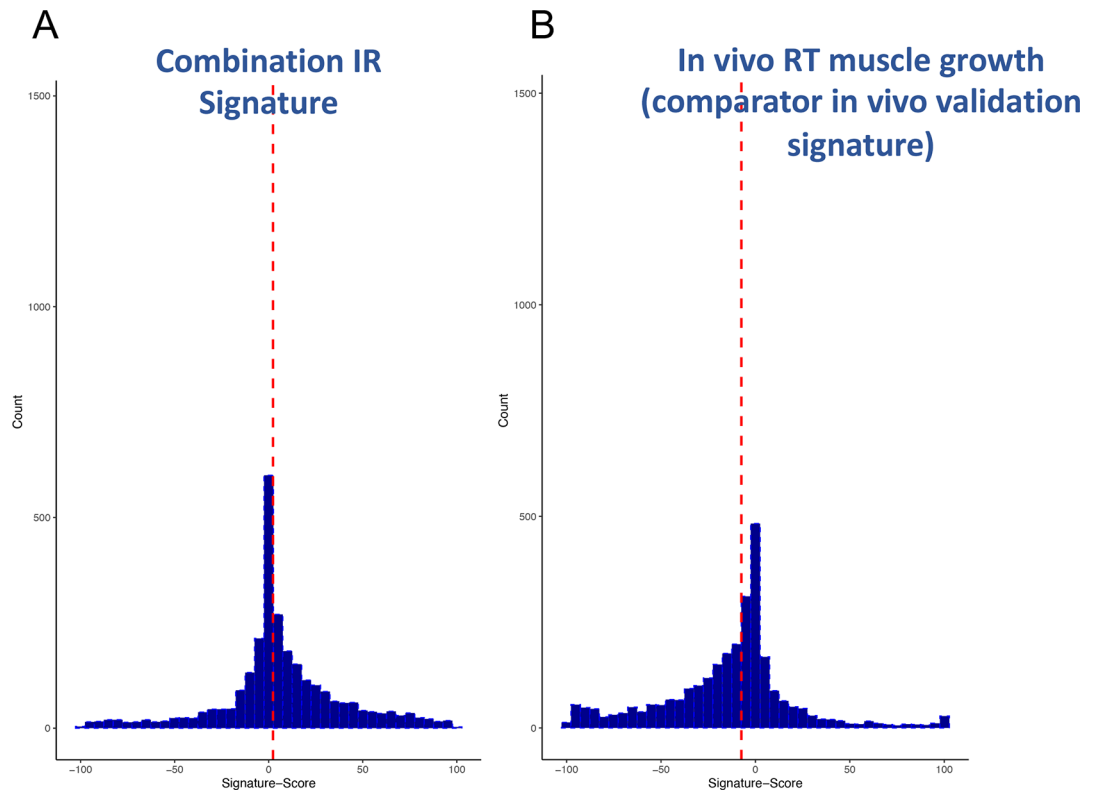Appendix figures (*Appendix 1—figures 1–11*).
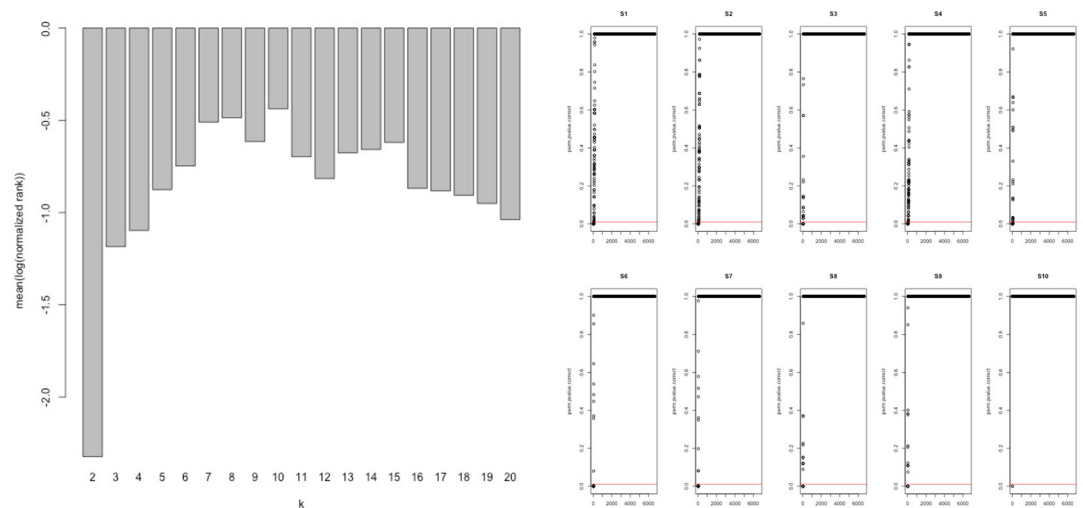
Appendix 1—figure 1. Network analysis statistics from MEGENA. Analysis of the combined 'disease' insulin resistance (IR) and 'treatment' response IR genes using tissue gene expression data (*Timmons et al., 2018*; *Timmons et al., 2019*) identified those genes that had the greatest connectivity in tissue. These values were used to re-rank and select the top 60 upregulated (positively correlating) and 60 downregulated (negatively correlating) genes regulated in common in adipose and muscle tissue (see Methods).
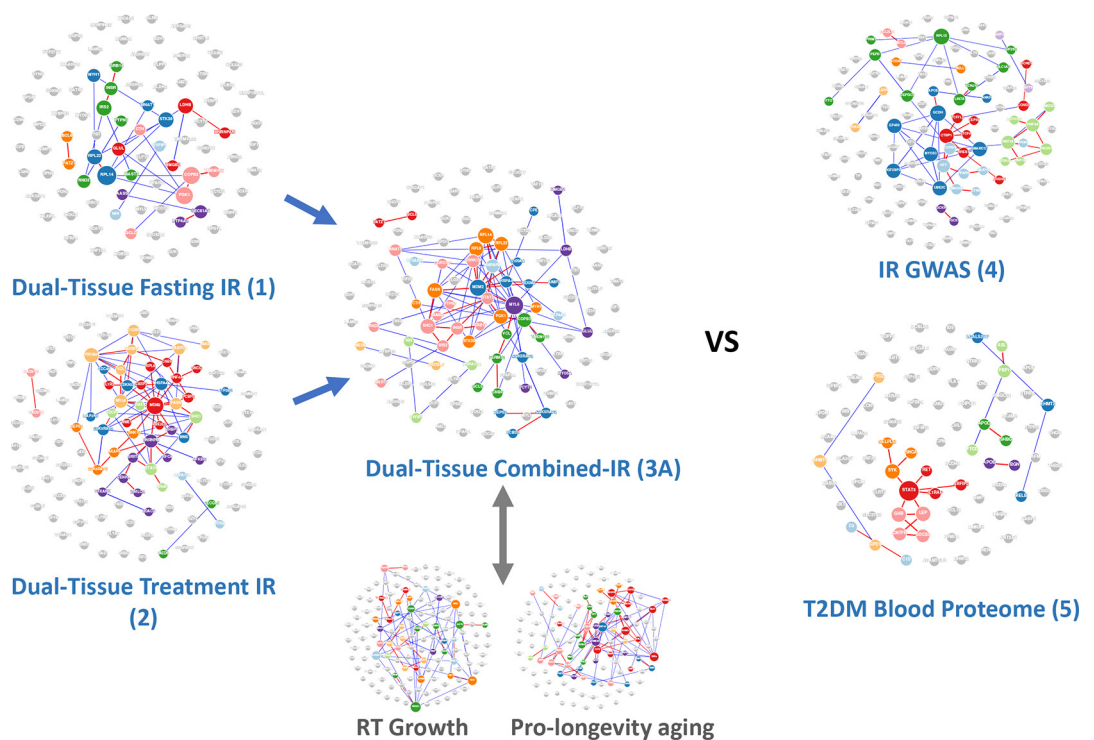

Appendix 1—figure 2. Network-based analysis of the gene lists from Table 1 analysed using protein-protein interaction data. A notable characteristic of these gene lists was that prior knowledge using multi-omic interaction databases (http://apps.broadinstitute.org/genets) was unable to connect the members of the list, indicating that previously unknown information was contained within each list

*Appendix 1—figure 2 continued on next page*

Appendix 1—figure 2 continued

and our novel analysis. There were <3% overlap of genes across the signatures considered in this study (Table S1) and only two genes common between signatures 3A and 4 (INSR, GRB14), and these were not essential for the performance of the RNA-based insulin resistance-drug repurposing (IR-DR) signature. See Figure S3 and 'Discussion' for reference to additional human signatures beyond IR.


Appendix 1—figure 3. Distribution of scores from clinical input signatures. Using the input gene lists from Table 1 and the CLUE dataset of >2500 compound signatures, the degree of match (-100 to +100) was established across nine cell types. (**A**) Distribution of scores was plotted and demonstrates that the majority of compounds are not significantly active. (**B**) For comparison, it can also be observed that a human muscle in vivo pro-growth signature (*Stokes et al., 2020*) yields an excess of negatively acting compounds, confirming as expected that the drug database may be biased for anti-tumour/anti-growth compounds.
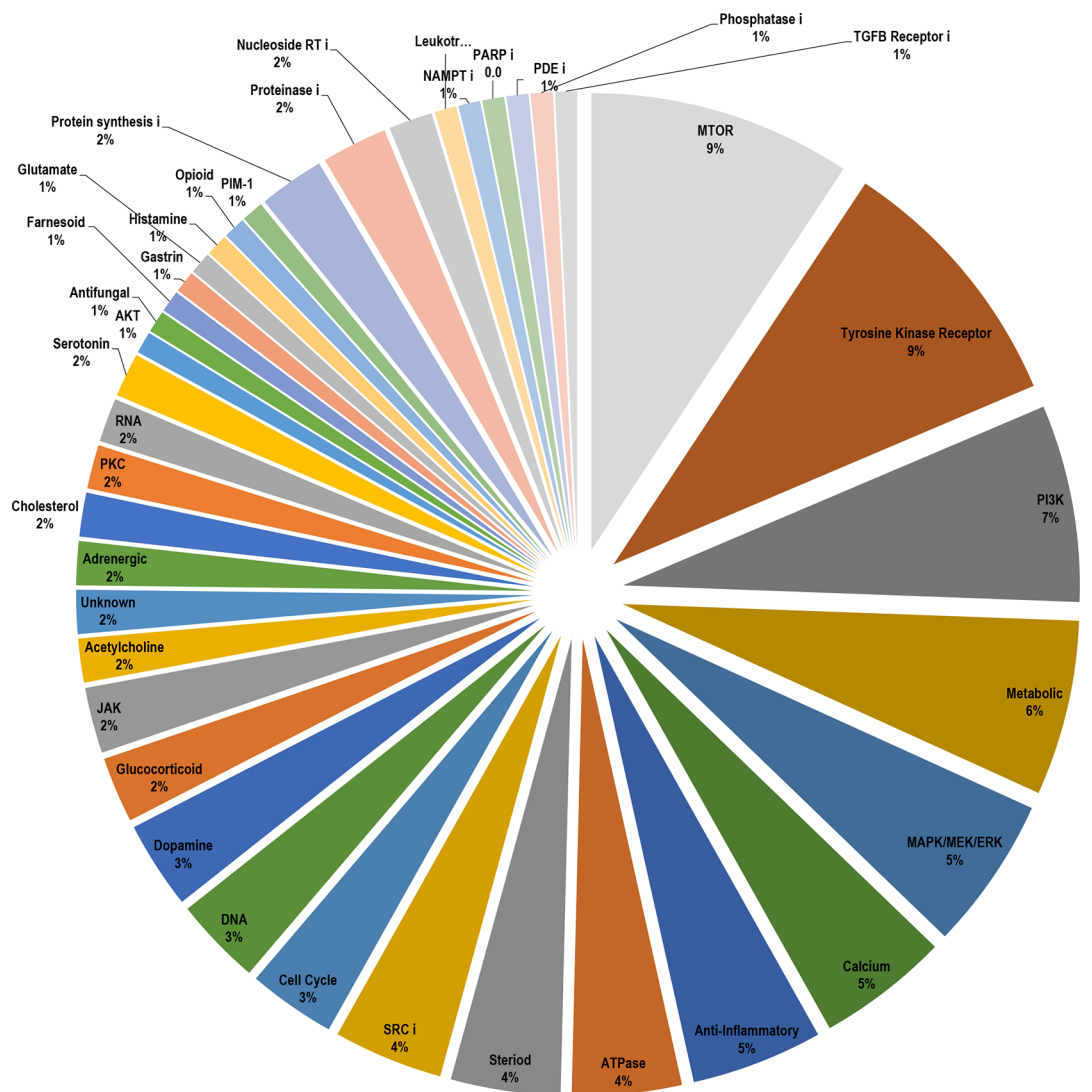
Appendix 1—figure 4. Breakdown of the drug classes of positive scoring insulin resistance-drug repurposing (IR-DR) compounds based on their known primary pharmacological actions. From >250 active compounds, 140 were associated with a positive action on the IR-DR signature and thus predicted to treat IR. Using the pre-assigned pharmacological descriptors of each compound, they were groups into general classes of compound and represented by a pie-chart. Over 45% of the compounds were classed as kinase inhibitors, while the remaining positively acting compounds belonged to a broad range of pharmacological classes
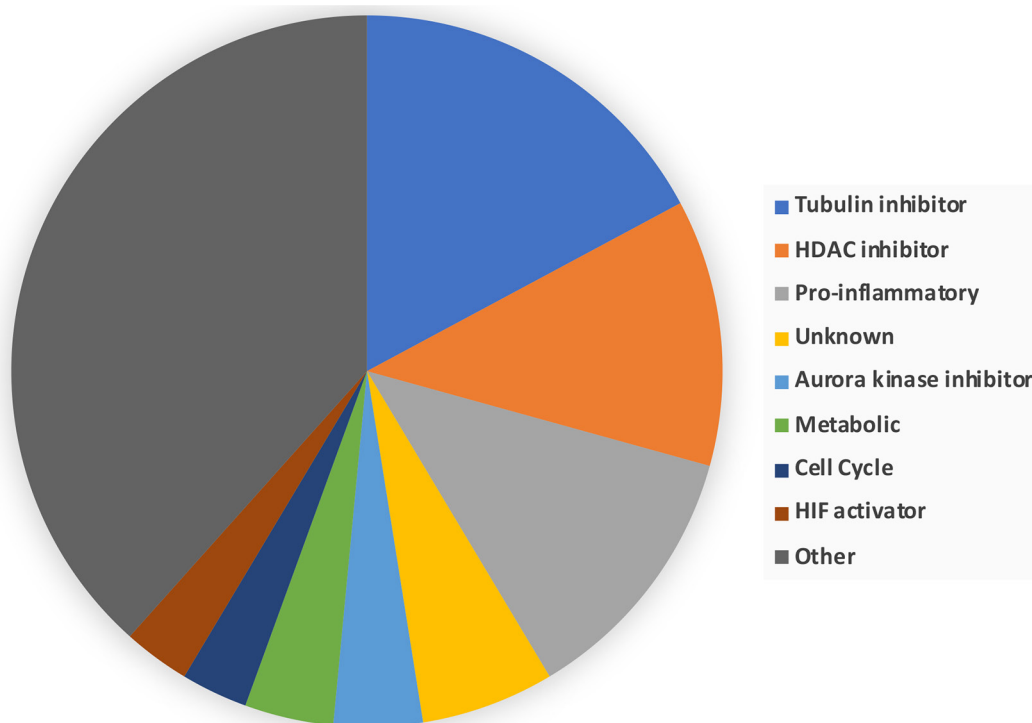
Appendix 1—figure 5. Breakdown of the drug classes of negatively scoring insulin resistance-drug repurposing (IR-DR) compounds. From >250 active compounds, ~100 were associated with a negative action on the IR-DR signature and thus predicted to aggravate IR. Using the pre-assigned pharmacological descriptors of each compound, they were grouped into general classes of compound. 17% of the compounds were classed as tubulin inhibitors, while the remaining compounds belonged to a relatively narrow range of pharmacological classes including compounds associated with activation of pro-inflammatory pathways and disruption of cell cycle.
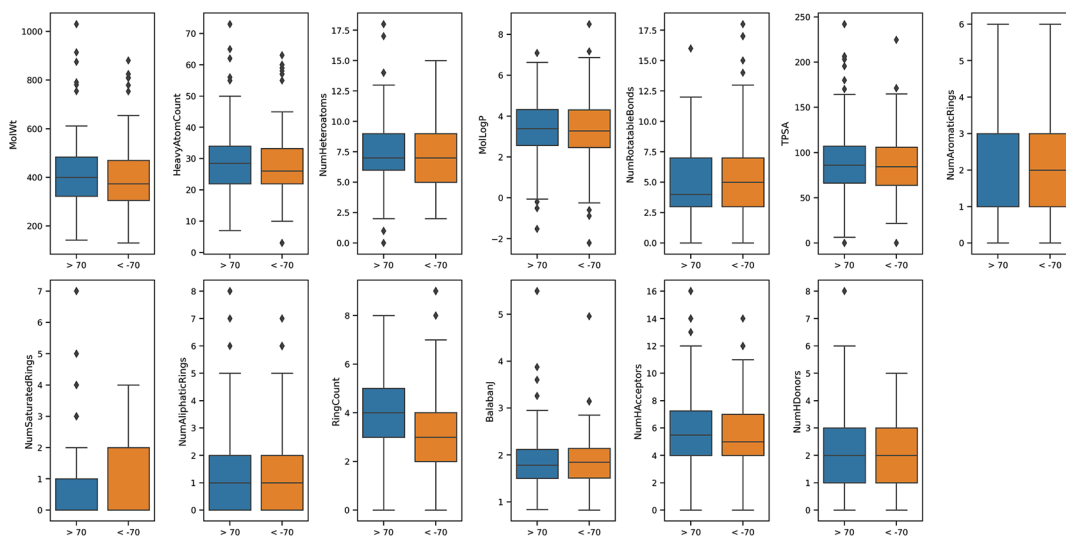
Appendix 1—figure 6. Calculated physicochemicals do not distinguish between positive and negative acting drugs. Calculated physicochemical descriptors (RDKit) were used to compare positively or negatively acting on the insulin resistance-drug repurposing (IR-DR) signature for systemic properties that might contribute to assay score (MolWt, HeavyAtomCount, NumHeteroatoms, MolLogP, NumRotatableBonds, TPSA, NumAromaticRings, NumSaturatedRings, NumAliphaticRings, RingCount, BalabanJ, NumHAcceptors, NumHDonors). The results were plotted using mean and standard deviation.

3799 RNAi KD of individual genes in vitro (6-9 cell types)

Novel 120* Gene IR-DR signature
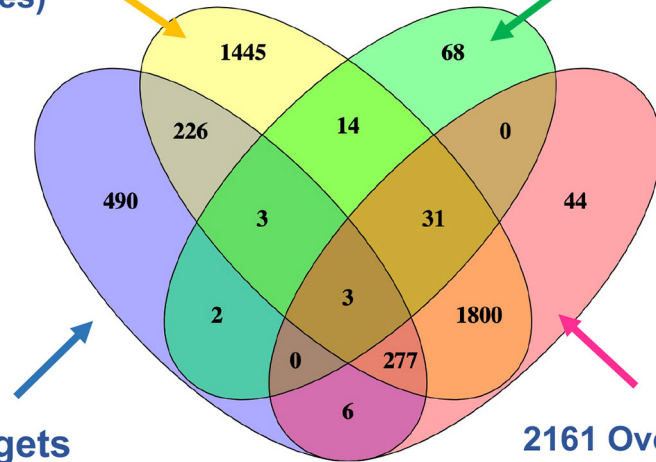
1007 Gene Targets derived from PubChem & CLUE annotations for active drugs

2161 Over-Expression of individual genes in vitro (6-9 cell types)

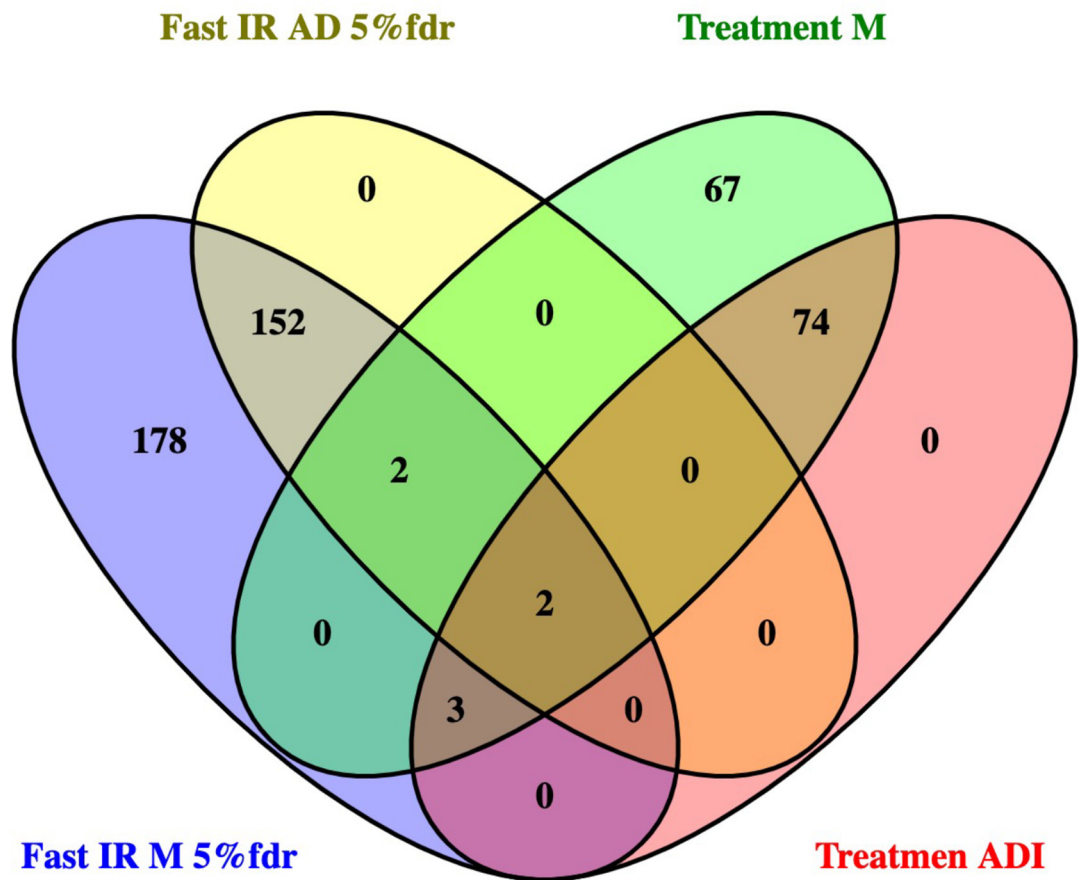**1 synonym is not consistently named in various studies*

Appendix 1—figure 7. Venn diagram overlap of putative drug targets. Comparison of drug signature, estimated protein targets of active drugs and knock-down (KD) and overexpression (OE) resources in CLUE that could be cross-compared with the insulin resistance-drug repurposing (IR-DR) signature.
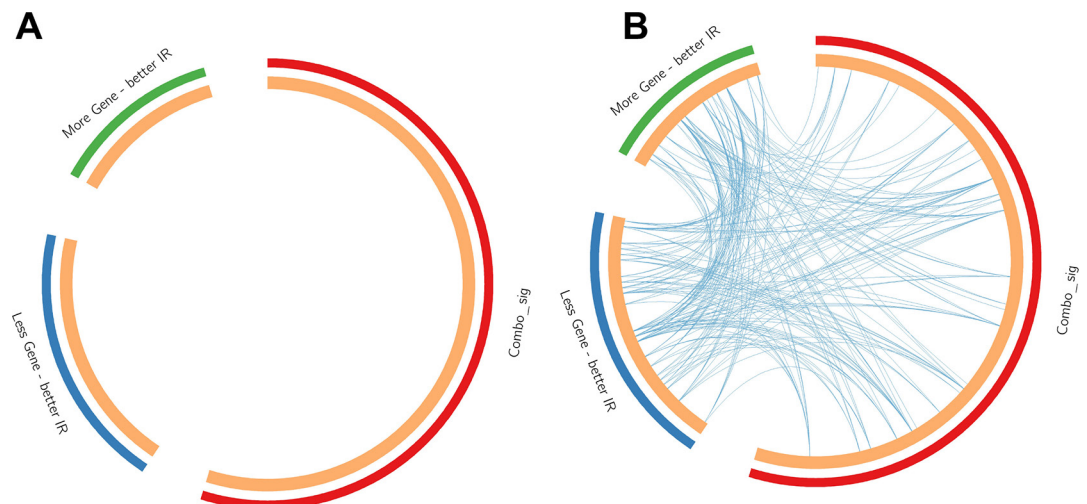
Appendix 1—figure 8. Contrast between gene list and pathway-level connections. Comparison of insulin resistance-drug repurposing (IR-DR) drug signature genes with 73 knock-down/overexpression (KD/OE) validated proteins from the positively acting IR-DR drug list. This demonstrates that while (**A**) no individual validated protein targets were in the drug repurposing signature, many belonged to pathways that contained the known drug targets (**B**). Blue lines connect common pathways.
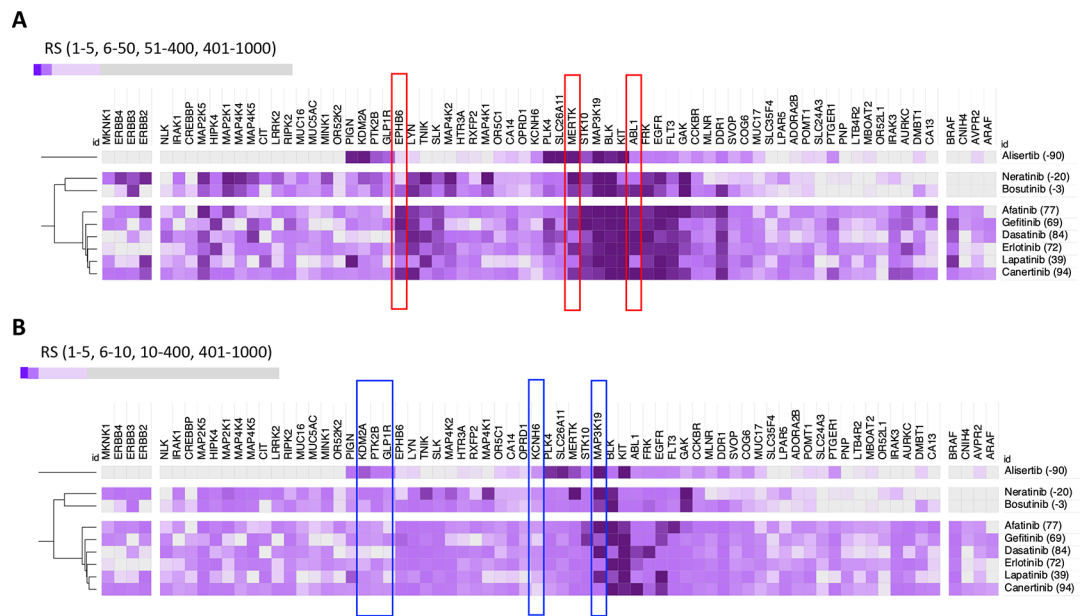
Appendix 1—figure 9. DeepPurpose-based target protein predictions. (**A**) Identification of predicted positive mediators of a positive insulin resistance-drug repurposing (IR-DR) score agrees with the pharmacological analysis. (**B**) Identification of predicted negatively acting proteins, diminishing the strength of a positive IR-DR score, or cancelling out any positive activity, agrees with and extends the known pharmacology.

Appendix 1—figure 10. Exploratory analysis of predicted protein target affinity. (A) Drugs that positively or negatively associate with the insulin resistance-drug repurposing (IR-DR) score applied to compounds with limited or no existing pharmacological data (other than for epidermal growth factor receptor [EGFR]). (B) Correlation between fusion rank score and IR-DR assay score for individual protein targets. For example, the more potent the predicted action was against MAP3K19 (smaller value) the poorer the IR-DR score was.

Appendix 1—figure 11. Transcripts related to HOMA2-IR, independent of donor chronological age, in muscle and adipose tissue. Primary analysis relied on identifying RNA that tracked with HOMA2-IR in muscle as this tissue represented the largest number of independent data sets – for both fasting tissue status and response to lifestyle intervention. Thereafter the candidates identified in muscle were examined in adipose tissue. The statistical 'significance' of the relationship (e.g. FDR < 5%), the magnitude and direction of the linear relationship (correlation coefficient) all informed the final selection of marker genes. As can be observed, in this analysis, the fasting HOMA2-IR genes and the treatment response HOMA2-IR genes represent a largely independent pool of genes (only VCL, GSTO1, SEC31B, FERMT2, OGFOD3, CENPV and NDUFAF5 were common to both states).